MAREES TERRESTRES

BULLETIN D'INFORMATIONS

130

1 DECEMBRE 1998

Association Internationale de Géodésie

Commission des Marées Terrestres

Editeur Dr. Olivier FRANCIS
Observatoire Royal de Belgique
Avenue Circulaire 3
1180 Bruxelles

BIM 130

1 décembre 1998

	p.
JOUSSET PH., MELCHIOR P., TJETJEP W., DUCARME B. Oceanic Tidal Gravity Loading in Java Island.	10030
BOYARSKY E.A., LATYNINA L.A. The analysis of the tidal parameters on short measurement intervals.	10050
URUCHADSE R.M., traduction Perturbations irrégulières de la dérive d'un extensomètre vertical en relation avec les variations de la pression atmosphérique.	10058
OZAWA I. Observations of the Earth Tide vertical extensions in the old Osakayama tunnel.	10064
MELCHIOR P. Vertical tidal strains in underground cavities.	10076
BALAVADZE B.K., ABACHIDSE V.G., KARMALEYEVA R.M., LATININA L.A., TSAGOURIA T.A., traduction Etude des déformations de marées de l'écorce terrestre selon les observations déformographiques à la station de Khoudoni.	10082
PERTSEV B.P., traduction Déformations de la surface de la Terre et variations du champ gravitationnel dues à la montée de la mer Caspienne.	10086
ABACHIDSE V.G., MELKADSE Y.A., traduction Analyse harmonique des inclinaisons de marées dans la région d'Ingouri.	10093
MELCHIOR P. The Kelvin Calibration Machine for Tilt.	10096

Oceanic Tidal Gravity Loading in Java Island

Ph. Jousset , P. Melchior*, W. Tjetjep**,.B. Ducarme*

1. Introduction

In the frame of the International Global Geodynamics Project (GGP) a group of Japanese Institutions has recently installed a «GGP Japanese network» of superconducting gravimeters which includes, amongst five other stations an equatorial station at Bandung, Java island (Indonesia). Two tidal gravity stations equipped with LaCoste-Romberg gravimeters operated previously in Java island : Bandung and Babadan (figure 1). A comparison of their results is therefore of present interest.

In paper entitled *«Tidal Gravity Measurements in Southeast Asia»* presented at the IAG Symposium «Geodesy in Southeast Asia» (Boulder IUGG General Assembly 1995) by Melchior, Francis and Ducarme, published later in the Bulletin d'Informations des Marées Terrestres 125, 1996 (hereafter referred as MFD), the authors discussed results obtained at 17 tidal gravity stations amongst which 7 are situated in Indonesian islands including the Bandung station which was equipped with the LaCoste Romberg gravimeter 336.

In the mean time the LaCoste Romberg gravimeter 131 model D installed at Babadan (Merapi volcano) in 1993 was equipped in 1994 with a electrostatic feedback by Van Ruymbeke (1991). New registrations started in october 1994 and 1235 days of registration presently available are analysed here.

2. Oceanic Tides

The area exhibits a quite complicate distribution of the M_2 oceanic tide with not less than 10 amphidromic points (see the reproduction of the Schwiderski M_2 cotidal map on MFD figure 3) while the O_1 oceanic tide has only 3.

However the presence of amphidromes results in low amplitude oceanic tides (see MFD Table 7). Typical values of the oceanic tides at harbours more or less close to our stations are :

South Coast of Borneo (Kalimantan)

Kotta Waring	2°54' S	111°24' E	M_2	22.0cm	O_1	16.0cm
Sungai Musang	3°30' S	114°30' E	M_2	28.8cm	O_1	27.3cm

* Observatoire Royal de Belgique
** Volcanological Survey of Indonesia

North Coast of Java

Djakarta	6°06' S	106°53' E	M_2	5.3 cm	O_1	13.5 cm
Semarang	7°00' S	110°24' E	M_2	4.7 cm	O_1	4.4 cm
Rembang	6°42' S	111°18' E	M_2	4.4 cm	O_1	15.2 cm
Surabaya	7°12' S	112°36' E	M_2	44.3 cm	O_1	27.2 cm

South Coast of Java

Tjilatjap	7°42' S	109°00' E	M_2	49.6 cm	O_1	11.7 cm

Along the north coast of Java the O_1 amplitude regularly increases from 4 cm to 25 cm towards the eastern extremity of the island while the M_2 amplitude is more variable, of the order of 5 cm up to Surabaya (7°12' S, 112°36' E) and between 30 cm to 50 cm from Surabaya to the East.

The north coast of Java and the south coast of Borneo (Kalimatan) are respectively the southern and northern boundaries of the shallow Java sea (two M_2 amphidromic points) while its south coast is a part of the northern boundary of the deep Indian Ocean.

A tentative improvement of the modelisation of ocean tides in Indonesian seas was performed by Mazzega and Bergé (1994) using Topex/Poseidon altimetry data.
As local constraint in their inversion scheme, they used only the tide gauge datas of Surabaya in Java and Bandjarmasin on Borneo island (figure 3c of their paper), obtaining apparently an M_2 amplitude of 20 cm at the eastern extremity of Java island and an amphidromic point north of Djakarta at φ = 4° South, λ = 107° East (rather close to Billiton island). The corresponding amphidromic point in Schwiderski model is at φ = 5° South, λ = 111°5' East) but there is also an M_2 amphidromic point at $\varphi \sim 6°$ South, $\lambda \sim 114°5'$ East on both models of Schwiderski and FES95.1 which does not appear on Mazzega-Bergé map.
However they used, in the Indonesian seas, not less than 76 tide gauge stations (not drawn on their figures) as an external data set for model comparisons and accuracy assessments.
They conclude that their solutions have an accuracy comparable to the Schwiderski and Cartwright-Ray models but that «beyond this qualitative agreement these models may present considerable localised discrepancies».

Matsumoto et al. (1995) also use Topex/Poseidon altimetry data to construct ocean tide models. The amplitude differences between their M_2 solution and the Schwiderski and TPX0.2 (Egbert et al. 1994) models are shown on their figures 3 and 5 which, despite their small size, let appear serious discrepancies in the Indonesian seas which could exceed 15 cm.
These authors emphasise the difficulties of modelisation in this area dues to shallow waters where bottom friction is important and to the limited resolution of 0.5° x 0.5° grid which is not able to express the rapidly varying tides around the Indonesian islands.
Ground based tidal gravity measurements which allow precise determinations of the oceanic loading effects could be used by an assimilation procedure to resolve these contradictions.
Matsumoto et al. compared indeed their models and the Schwiderski and TPX 0.2 (Egbert et al.) models as well with the results of to superconducting gravimeters installed by japanese institutions at Syowa in Antarctica and at Esashi in the north of Hondo island in Japan.

Melchior and Francis (1996) compared several recent ocean tide models using ground-based tidal gravity measurements at world scale. They concluded that «for assimilation purposes one has to take into consideration that stations which are too remote from the ocean do not allow to discriminate the different solutions, while on-shore stations may be considerably disturbed by strong local shelf tides and the difficulty of calculating the Green's function correctly. An optimum distance range is from 20 km to 150 km». (Bandung and Babadan stations fulfil this criterion as they are distant by about 70 km from both Java coasts).
For what concerns the South East Asia area, their Table 10 shows that, for the 19 tidal gravity stations concerned, the amplitudes of the final residues X obtained after vectorial subtraction of the calculated oceanic loading are considerably decreased with respect to the observed residue amplitudes B for the tidal wave O_1 while the results for the tidal wave M_2 are not so satisfactory.

For example, for three stations established on both sides of the Java sea they obtained, with the Schwiderski model, residual amplitudes of the same size for O_1 and M_2 waves i.e., expressed in microgals :

			O_1			M_2		
			B	X	X/B	B	X	X/B
4105 Banjar Baru	3°20' S	114°47' E	2.23	0.42	0.19	1.79	0.94	0.53
4100 Bandung	6°54' S	107°38' E	1.46	0.29	0.20	4.84	2.51	0.52
4110 Ujung Pandang	5°40' S	119°38' E	2.73	0.54	0.20	3.48	3.33	0.96

(4105 South Coast of Kalimantan / Borneo)
(4110 Macassar, Sulawesi / Celebes)

The very satisfactory results obtained for the O_1 wave demonstrate that the large M_2 residues are not due to a calibration instrumental effect but to imperfections of the modelisation of the complicate M_2 wave patterns in the Indonesian seas.

3. The «Solid Earth Tide» Models

The most recent theoretical developments by Dehant, Defraigne and Wahr (1998) show that the latitude dependence of the amplitude factor δ ($\delta = 1 + h - 3/2k$; h, k are the elastic Love numbers), due to the Earth's flattening and the Coriolis force is very weak.
One can therefore adopt for all the stations concerned here values calculated for the latitude of Babadan, 7°32' South :

$$\delta (O_1) = 1.15410 \quad \text{or} \quad 1.15272$$
$$\delta (M_2) = 1.16164 \quad \text{or} \quad 1.16025$$

respectively corresponding to an inelastic, non hydrostatic model and to an elastic hydrostatic model.

The effect of inelasticity is extremely small for what concerns the phase lag which remains unobservable in the present circumstances (Dehant et al. 1998).

4. The tidal gravity stations

4.1. Babadan station 4103

The Babadan station has been installed for 3 objectives :

1) to give data for improving global Earth tides models and especially for better understanding the oceanic loading in south-east Asia;
2) to obtain an accurate local Earth tide model for corrections to volcanic repeated microgravity measurements;
3) to better understand processes linked to gravity changes within volcanoes.

This paper addresses the first and second point, whereas the second point has already been addressed in Jousset, 1996 and Jousset et al. (in press) and the third point is addressed elsewhere.

The gravimeter LaCoste-Romberg D131 (Volcanological Survey of Indonesia) has been installed in november 1993 at 4 km from the active crater of Merapi volcano (3000 m high). The station (7° 32' S, 110° 25' E, 1378 m) is installed at the Babadan observatory post in the bunker built during Dutch ruling to protect observers from nuées ardentes. It is equipped with a number of other instruments designed for volcanic monitoring and meteorological data recording (pressure, humidity and temperature). The gravimeter is installed on an heavy pillar in a seismically quiet place and in a thermostatized room (less than 1° C temperature variation over the year). The gravimeter is enclosed in a protective box to further reduce external temperature variations. Data are stored in a PC through a microDAS (Van Ruymbeke et al., 1997).

In August 1994, electrostatic feedback nulling has been fitted to the gravimeter, in particular for the reduction of the tilt effects on the gravimeter sensibility. The present analysis uses data from october 1994 to april 1998. Careful calibrations have been regularly conducted (Jousset et al., 1998, in press).
The analysis of a series of 1235 days of registration is reproduced in the Table I.

4.2. Bandung station 4100

The Bandung station was established in 1976 in the frame of the Trans World Tidal Gravity Profiles initiated by the Royal Observatory of Belgium and the International Centre for Earth Tides with the cooperation of the Indonesian National Committee of Geodesy and Geophysics (prof. Jacub Rais).
The instrument used during 215 days was the LaCoste Romberg model G, 336 installed on a specially built heavy pillar in a thermo-isolated underground room of a building of the Geological Survey of Indonesia.
The analysis of a series covering 215 days of registration is reproduced in the Table II.

5. Results obtained for the M_2 and N_2 semi diurnal sectorial lunar waves.

Sectorial waves are maximum at the equator for gravity variations : the M_2 wave amplitude reaches 88 µgal at Babadan and Bandung thus a peak to peak gravity variation of 176 µgal. The oceanic loading reaches 4.5 µgal i.e. 5% of the observed amplitude.

Two oceanic models were used by MFD, the Schwiderski 1980 (classical) models and the FES95.2 models (Le Provost).

FES models are constructed by the finite elements method (see Fig. 2) thus with a much narrower grid points than the Schwiderski 1° x 1° models. *«One could expect therefore some improvement in the description of the tides around the many islands of Indonesia, notably in the Java sea, Banda sea, and the Timor and Savu seas»* according to MFD.

The meandering line connecting the M_2 amphidromic points separates the 17 stations into two groups : those in the south - south west and those in the north - north-east of the line as shown in the MFD Table 6.
Babadan station as well as Bandung station pertains to the first group.

Five oceanic models are used here : Schwiderski, CSR3.0, FES95.1, ORI and ORI 96.

The results of both stations are compared in the Table III. The agreement between the observed tidal factors δ, α and the B vectors (observed M_2 vector minus «solid» Earth Model M_2 response) is quite good.
B vectors exhibit a 4.5 µgal large amplitude with comparable negative phases.
The consideration in MFD that *«the mean difference 0.6 µgal and a phase around -150°»* between the Schwiderski and FES95.2 oceanic loadings is, as expected, almost perfectly confirmed at the new station Babadan.

The CSR3.0 oceanic model seems to better represent the M_2 oceanic tides around Java island as it gives the smallest final residues X, 0.76 µgal at Babadan and 1.92 µgal at Bandung but corrected phases α^* disagreing between Bandung and Babadan.
On the contrary, the FES.95.1 model gives corrected δ^* and α^* values more coherent for the two stations while the Table VIII exhibits a lack of agreement in the phases differences β and λ between the two stations.
Similar conclusions are obtained for the lunar elliptical wave N_2, results (amplitude 17 µgal) given in the Table IV : excellent agreement of the two stations for the observed parameters δ, α and the B vectors. The Table VIII exhibits phases differences β and λ between the two stations in fair agreement for such small vectors.

However, for both stations, the oceanic corrections applied when using five different models, do not bring the δ, α values close to those of the solid earth models, even if the correction to the observed high values of δ is important and in the correct sense of a decrease. Also the strong negative phases are decreased by a large amount (at the exception of the wave N_2 at Bandung). This is due to imperfections in the oceanic models. The observed small phase difference between Bandung and Babadan, + 0.15° only, is indeed reversed and increased to about - 0.70°

Nevertheless the four new models give amplitude factors δ^* which are lower respectively by 0.7% and 1% than the Schwiderski model for M_2 and N_2 components.

6. Results obtained for the O_1 diurnal tesseral lunar wave.

The diurnal waves vanish at the equator for gravity : the theoretical O_1 wave amplitude reaches respectively 8.5 and 9.3 µgal at Bandung and Babadan while the oceanic loading reaches about 1.5 µgal at Bandung and 2 µgal at Babadan i.e. 20% of the observed amplitude.

The B vectors measured at both stations are in almost perfect agreement (Table V). The concordance between the phases β and λ (Table VIII) is impressive for B and L vectors of 2 µgal amplitude. Thus it is not astonishing that the final residue vectors X have an amplitude of 0.25 µgal, of the order of the local and instrumental noise.

The oceanic loading has also been calculated with five models : Schwiderski, CSR3.0, FES95.1, ORI and ORI 96.
However, due to the small theoretical amplitude of the diurnal waves in the vicinity of the equator, the oceanic corrections do not allow to obtain δ, α parameters in good agreement with the «solid earth tides» models, despite the apparent coincidence of the B and L vectors : a difference of 0.05 µgal on B or L would be sufficient to bring the δ (O_1) value equal to its «model» value 1.1541.
Again in the case of the O_1 diurnal wave, the FES95.1 model gives corrected δ^*, α^* values and, consequently, final residues X more coherent for the two stations.
As a matter of fact the observed vectorial difference of the residues B between the two stations coincides exactly with the vectorial difference of the FES95.1 loading vectors L (Table VIII). In this respect the ORI model does not appear to be satisfactory for the O_1 wave.

The better fit of the data at the O_1 frequency may be attributed indeed to the less turbulence of the oceanic waves (only one amphidromic point at the northern coast of Java).

7. Solar waves S_1, S_2 and Atmospheric Pressure

Atmospheric pressure and temperature effects are responsible for the existence of a non-tidal S_1 frequency in the diurnal band and for perturbations of the S_2 tidal frequency in the semi-diurnal band.

At the S_1 frequency one has observed (see Tables I and II)

at Bandung	$B = 1.8 \pm 0.50$ µgal	$\beta = 113° \pm 15°$
at Babadan	$B = 0.9 \pm 0.06$ µgal	$\beta = 116° \pm 4°$
at Banjar Baru	$B = 1.4 \pm 0.25$ µgal	$\beta = 123° \pm 10°$

which are in fair agreement despite of the larger mean square errors at Bandung, due to the fact that the observation period do not reach one year but only 215 days.
It is well known that the S_1 atmospheric tide is very irregularly distributed over the globe, being clearly «associated with the continents - oceans distribution owing to the different thermal and thermodynamic qualities of land and water masses» (Elstner 1995) and present large seasonal variations. However at the daily solar frequency the temperature variations can be coherent and produce similar effects in stations situated in the same equatorial area.

On the contrary the S_2 atmospheric tide is known to be very regular and to obey the empirical law

$$S^2_2(p) = 1190 \cos^3 \varphi \cos(2\tau - 111°) \text{ µbar} \quad \text{(Siebert 1961)}$$

We had no atmospheric pressure data to correct the Bandung results but for Babadan a series of more than three years could be analysed, giving

at S_1 frequency

465 ± 15 µbar $\quad -89.5° \pm 1.8°$

and at S_2 frequency

906 ± 5 µbar $\quad -110.3° \pm 0.3°$

which looks in quite good agreement with the empirical law.

On the other hand, the admittance coefficient relating atmospheric pressure loading to gravity change is generally comprised between - 0.28 and - 0.39 depending if we accept the inverted barometer (IB) above the sea areas or not (NIB). With a supposed coefficient - 0.35 at Babadan, the atmospheric pressure would give a contribution of 0.32 µgal with a phase + 70° but this does not cancel the X residues neither at Babadan or Bandung even if this phase corresponds to the $\chi(S_2)$ phase at Bandung (Table VI).

The contribution of the atmospheric pressure variations to the S_1 and S_2 frequencies considerably disturbs the results obtained for the luni solar and solar waves K_1, P_1 (being yearly modulations of S_1) and S_2.
For the semi diurnal solar wave S_2 (amplitude 40 µgal) phases observed (Table VI) are + 2.98° at Bandung and - 3.08° at Babadan, a difference of 6° which cannot be explained in terms of purely tidal effects.

For the diurnal luni solar wave K_1 (amplitude 13 µgal) the difference of the α phases is 7° between Bandung and Babadan (Table VII). Only an analysis of atmospheric pressure variations at the epochs of tidal gravity measurements could help to explain such differences. But pressure data are not presently at our disposal for Bandung while the pressure data at Babadan give a very small K_1 component (see above) corresponding to only 0.14 µgal.

8. Conclusions

The two stations have been established respectively in 1976 and in 1994, by two different teams, using two different LaCoste Romberg instruments.
The stations are about 300 km apart and both are distant by about 70 km from both coasts of the island. Their altitudes are high, respectively 714 and 1378 meters.
The coherence of the results (observed δ, α parameters and B residues) obtained for the purely lunar waves M_2, N_2 and O_1 is remarkable even if the diurnal wave O_1 has a small amplitude (9 µgal only), a normal situation for a quasi equatorial station.
This shows that the calibrations of the two instruments in amplitude and in phase have been correctly performed.
The correction for oceanic attraction and loading is obviously a difficult operation in an area comprising many large islands which produces a most complicate pattern of cotidal - corange lines.
The results obtained for these three lunar waves indicate a general preference for the FES 95.1 model even if the differences are small in terms of amplitude.
Melchior (1995) has shown that correlations with tectonic features are not excluded in the tidal gravity results. The concerned parameter is here the M_2 residue projection X cos χ which exhibits a correlation with heat flow provinces. Both stations, Bandung and Babadan exhibit indeed large positive values for X cos χ, respectively + 2.0 and + 1.1 µgal (mean values of the five oceanic models), the measured heat flow at Bandung being 82 milliwat m^{-2} which seem to confirm this hypothesis.

Eight stations have been installed up to now in Indonesia (3 in Java, 1 in Kalimantan, 2 in Sulawesi, 1 in Timor and 1 in Irian Jaya) but, considering the considerable extension of the archipelago and the complicate pattern of the oceanic tides, additional stations would be necessary to improve the models, namely in Sumatera (to fulfil the gap with the 2 Malaysian stations), Kalimantan (Pontianak, Balikpapan), Sumbawa, Flores and Ceram provided a 20-50 km distance to the sea can be obtained.

9. Acknowledgments.

M. Diament was the instigator of the Merapi project. He also helped together with S. Dwipa and F. Beauducel for the station installation. Station maintenance and calibrations have been made by Mas Yulanto, Mas Nurudin, F. Bauducel, M. Dejean, J. Guilbert, T. Seligman. This work has been supported by the Délégation aux Risques Majeurs (Ministère de l'Environnement) and the French Embassy in Jakarta.

We are pleased to thank O. Francis for his calculations of tidal loading effects performed on the basis of five oceanic tides models and L. Vandercoilden for the analysis of the gravimetric and atmospheric pressure registrations, both at the Royal Observatory of Belgium.

References

Dehant, V., Defraigne, P. and Wahr, J-M., 1998
Tides for a convective Earth.
Journal of Geoph. Res. (accepted, in press).

Elster, C., 1995
Seasonal variations of the Planetary Solar Air Pressure Waves.
Bull. Inf. Marées Terrestres 122, 9202-9211.

Jousset, P., 1996
Gravimétrie et microgravimétrie en volcanologie : méthodologie et application au volcan Merapi, Java, Indonésie.
Ph.D. Univ. Paris VII - IPGP.

Jousset, P., Dwipa, S., Beauducel, F., Duquesnoy, T. and Diament, M., 1998.
Temporal gravity at Merapi during the 1993-1995 crisis : an insight into the dynamical behaviour of volcanoes.
J. Volcanol and Geoth. Res., in press, special Volume Merapi Decade I.

Mazzega, P. and Bergé, M., 1994.
Ocean tides in the Asian semi enclosed seas from TOPEX/POSEIDON.
Journal of Geoph. Res. 99, C12, 24867-24881.

Matsumoto, K., Ooe, M., Sato, T. and Segawa, J., 1995.
Ocean tide model obtained from TOPEX/POSEIDON altimetry data.
Journal of Geoph. Res. 100, C12, 25319-25330.

Melchior, P., 1995.
A continuing discussion about the correlation of tidal gravity anomalies and heat flow densities.
Physics of the Earth and Planetary Interiors, 88, 223-256.

Melchior, P., Francis, O. and Ducarme, B., 1996.
Tidal Gravity Measurements in Southeast Asia.
B.I.M. 125, 9493-9508.

Melchior, P. and Francis, O., 1996.
Comparison of Recent Ocean Tide Models using Ground-Based Tidal Gravity Measurements.
Marine Geodesy 19, 291-330.

Siebert, M., 1961.
Atmospheric Tides.
Advances in Geophysics, 7, 105-187.

Van Ruymbeke, M., 1991.
A new feedback system for instruments equipped with a capacitive transducer.
Proc. 11th Symposium on Earth Tides, Helsinki 1989.
Schweizerbartsche Verlagsbuchhandlung Stuttgart, 51-60.

Van Ruymbeke, M., Beauducel, F., Somerhausen, A., 1997.
The Environmental Data Acquisition System (EDAS), developed at the Royal Observatory of Belgium.
Cahiers Centre Eur. Géod. et Séism. 16 : 163-174.

Notations used

For the concerned wave (M_2, N_2, O_1 etc.)

δ, α : observed amplitude factor and phase

δ^*, α^* : amplitude factor and phase corrected for oceanic tidal loading.

A (A, α) is the observed vector

R (R, o) is the elastic oceanless earth model calculated response

B (B, β) = A - R

L (L, λ) is the oceanic attraction and loading calculated vector for the concerned oceanic model

X (X, χ) = B - L = A - R - L is the final residue

The amplitudes A, R, B, L, X are given in microgals.

The phase α, β, λ, χ are given in degrees, a minus corresponds to a lag (1° corresponds to 4.30 min of time for the wave O_1 and to 2.07 min of time for the wave M_2).

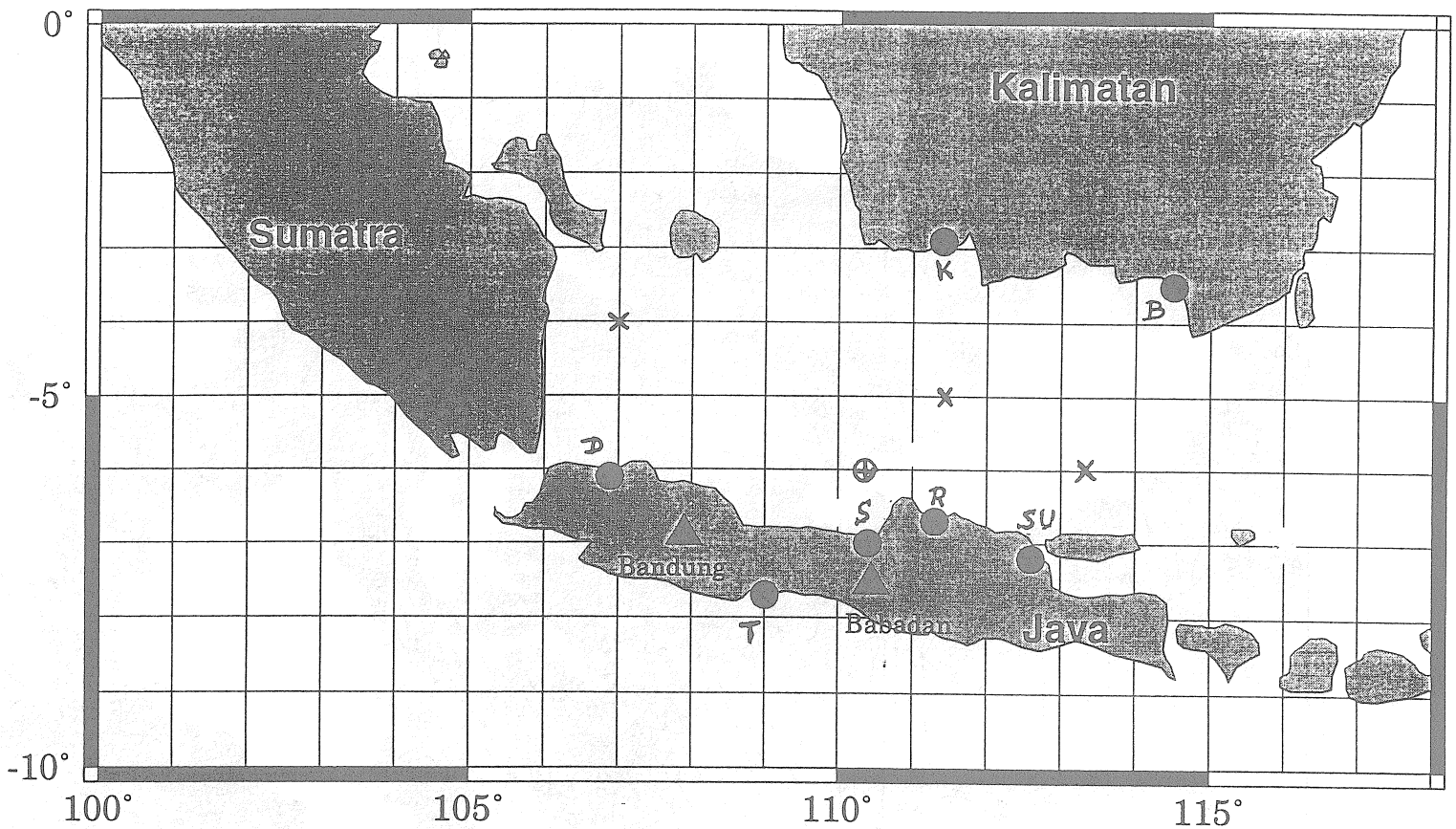

FIGURE 1: Distribution of sea tide gauges and amphidromic points in the Java Sea.

B: Banjar Baru/Sungai Musang
D: Djakarta
K: Kotta Waring
R: Rembang
S: Semarang
SU: Surabaya
T: Tjilatjap

⊕ O_1 amphidromic point
x M_2 amphidromic points

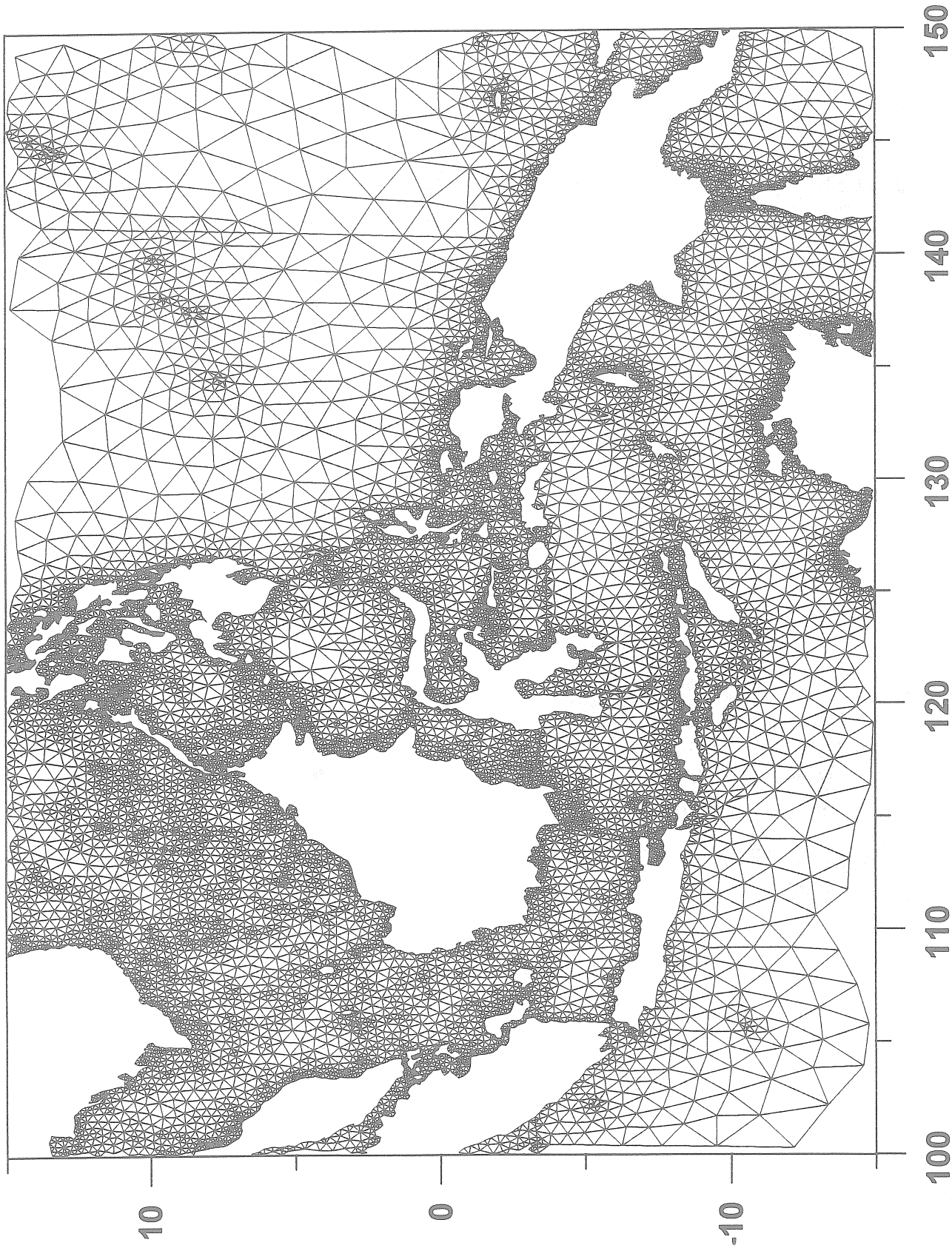

FIGURE 2 : Finite Element Mesh drawn by O. Francis on the basis of the Le Provost et al. model (1995) (courtesy of O. Francis)

Table I

STATION 4103 BABADAN/MERAPI INDONESIE

7.52610 S 110.41061E H 1378.M G= 977850.
GRAVIMETRE LA COSTE ROMBERG D131
CALIBRATION CONSTRUCTEUR
INSTALLATION M.DIAMENT,F.BEAUDUCEL,PH.JOUSSET
MAINTENANCE MAS YULANTO, MAS NURUDIN, F.BEAUDUCEL, M.DEJEAN
J.GUILBERT, T.SELIGMAN

LEAST SQUARE ANALYSIS / VENEDIKOV FILTERS ON 48 HOURS / PROGRAMMING B.DUCARME
POTENTIAL TAMURA COMPLETE DEVELOPMENT
COMPUTING CENTER INTERNATIONAL CENTER FOR EARTH TIDES/FAGS/ BRUSSELS
DATA PROCESSING BY B.DUCARME ON 98/07/29
COMPUTER HP-UX 9000/819
INERTIAL CORRECTION NOT APPLIED

RESIDUES COMPUTED WITH RESPECT TO MODEL DEHANT-DEFRAIGNE-WAHR:
non-hydrostatic inelastic model 1997

G131 941015/941027 9411 4/941112 941119/941127 9412 1/941225 95 1 6/95 116
G131 95 120/95 126 95 130/95 2 1 95 2 5/95 2 5 95 2 9/95 211 95 216/95 228
G131 95 3 5/95 3 5 95 3 8/95 312 95 317/95 412 95 416/95 418 95 428/95 428
G131 95 5 1/95 5 3 95 5 8/95 512 95 517/95 6 8 95 611/95 7 9 95 713/95 717
G131 95 730/95 8 3 95 8 7/9510 2 96 727/96 828 961117/9612 7 961221/97 217
G131 97 226/97 419 97 424/97 514 97 523/97 527 97 7 2/97 712 97 716/97 726
G131 97 730/97 8 7 971225/98 126 98 211/98 217 98 221/98 3 1

TIME INTERVAL 1235.5 DAYS 13536 READINGS 34 BLOKS EFFICIENCY 0.46

WAVE GROUP ARGUMENT	N	WAVE	ESTIMATED AMPL. R.M.S.	AMPL. FACTOR	R.M.S.	PHASE DIFF.	R.M.S.	RESIDUE AMPL.	PHASE
127.-12A.	20	SIGMA1	0.225 0.052	0.91240	0.20915	24.6223	13.1516	0.123	-49.54
133.-136.	33	Q1	1.798 0.053	1.16575	0.03436	16.9117	1.6870	0.526	-83.55
137.-13A.	18	RO1	0.417 0.047	1.42373	0.15975	30.5961	6.4252	0.213	-95.66
142.-145.	32	O1	9.387 0.049	1.16532	0.00612	12.2824	0.3008	2.001	-86.53
152.-155.	30	NO1	0.678 0.026	1.06943	0.04108	2.7764	2.2015	0.063	-31.32
160.-163.	17	P1	4.621 0.040	1.23297	0.01075	12.4559	0.5016	1.018	-101.69
164.-164.	4	S1	0.896 0.058	10.11092	0.64989	-57.7417	3.6257	0.846	116.43
165.-169.	35	K1	14.104 0.046	1.24489	0.00404	11.9572	0.1855	3.068	-107.72
174.-177.	25	J1	0.925 0.056	1.45985	0.08813	14.8402	3.4619	0.287	-124.30
184.-187.	23	OO1	0.571 0.074	1.64701	0.21337	11.1004	7.4283	0.194	-145.45
233.-236.	23	2N2	2.332 0.039	1.24863	0.02072	1.3201	0.9526	0.169	18.54
237.-23A.	21	MU2	2.801 0.039	1.24258	0.01722	-0.8487	0.7944	0.185	-12.97
242.-245.	25	N2	17.257 0.038	1.22242	0.00267	-1.6083	0.1253	0.969	-30.00
246.-249.	25	NU2	3.264 0.038	1.21739	0.01421	-1.4558	0.6666	0.168	-29.58
252.-259.	56	M2	88.587 0.037	1.20145	0.00050	-2.1088	0.0240	4.304	-49.23
264.-268.	32	L2	2.448 0.037	1.17483	0.01776	-1.8001	0.8681	0.081	-72.37
270.-273.	9	T2	2.474 0.038	1.23332	0.01899	-4.8196	0.8861	0.247	-57.33
273.-273.	7	S2	39.702 0.039	1.15734	0.00112	-3.0750	0.0564	2.143	-96.29
274.-278.	28	K2	10.749 0.050	1.15264	0.00533	-3.2370	0.2648	0.617	-100.21
315.-3A5.	82	*M3	1.534 0.010	1.06908	0.00686	-0.7452	0.3693	0.021	-111.40

STANDARD DEVIATION D 2.962 SD 2.791 TD 0.746 MICROGAL

QUALITY FACTORS : Q1= 3.2 Q2= 10.7
O1/K1 0.9361 1-O1/1-K1 0.6751 M2/O1 1.0310
CENTRAL EPOCH TJJ= 2450257.2

Table II

TRANS WORLD PROFILE INDONESIA STATION BANDUNG

STATION 4100 BANDUNG VERTICAL COMPONENT JAVA - INDONESIA
06 53 47 S 107 37 54 E H 714 M P 3 M D 70 KM G 977 991
UNDERLAYER OF VERY THICK VOLCANIC DEPOSIT OF SAND & OTHER VOLC.PRODUCTS
IUGG NATIONAL COMMITTEE PROF.J.RAIS GEOLOGICAL SURVEY OF INDONESIA
GRAVIMETER LACOSTE-ROMBERG 336 P.MELCHIOR TRANS WORLD PROFILES
CALIBRATION BRUXELLES-FUNDAMENTAL STATION
INSTALLATION B.DUCARME
MAINTENANCE M.UNTUNG/Y.JOYODIWIRYO/BUNDAN MUBROTO
GRANT AFOSR-73-2557A PROJECT-TASK 8607-02

LEAST SQUARE ANALYSIS / VENEDIKOV FILTERS ON 48 HOURS / PROGRAMMING B.DUCARME
POTENTIAL TAMURA COMPLETE DEVELOPMENT
COMPUTING CENTER INTERNATIONAL CENTER FOR EARTH TIDES/FAGS/ BRUSSELS
DATA PROCESSING BY B.DUCARME ON 98/11/12
COMPUTER HP-UX 9000/819
INERTIAL CORRECTION NOT APPLIED
NORMALISATION FACTOR .98662
PHASE LAG O1 .470 M2 .580 O1/M2 .810
CORRECTION FOR DIFFERENTIAL ATTENUATION M2/O1 1.00656 /MODEL 2/

RESIDUES COMPUTED WITH RESPECT TO MODEL DEHANT-DEFRAIGNE-WAHR:
non-hydrostatic inelastic case

G336 76 411/76 421 76 425/76 5 3 76 5 7/76 5 7 76 512/76 522 76 525/76 6 4
G336 76 6 8/76 618 76 624/76 624 76 627/76 629 76 7 2/76 7 4 76 7 7/76 917
G336 76 921/7610 9 761013/761110

TIME INTERVAL 215.0 DAYS 4656 READINGS 12 BLOKS EFFICIENCY 0.90

WAVE GROUP ARGUMENT	N	WAVE	ESTIMATED AMPL. R.M.S.	AMPL. FACTOR	R.M.S.	PHASE DIFF.	R.M.S.	RESIDUE AMPL.	PHASE
133.-136.	33	Q1	1.866	0.265	1.31787	0.18714	15.0871	8.1045	0.514	-109.04
142.-145.	32	O1	8.516	0.247	1.15122	0.03338	9.7806	1.6557	1.454	-84.27
152.-155.	30	NO1	0.608	0.122	1.04434	0.20910	11.5914	11.5022	0.144	-58.08
160.-163.	17	P1	4.820	0.211	1.40036	0.06133	20.0634	2.5046	1.749	-109.07
164.-169.	39	S1K1	12.513	0.228	1.20285	0.02196	8.7013	1.0462	1.972	-106.27
174.-177.	25	J1	0.608	0.278	1.04457	0.47729	-5.5274	26.2335	0.090	40.73
184.-187.	23	OO1	0.313	0.315	0.98185	0.98829	37.4253	57.6166	0.225	-57.76
233.-23A.	44	2N2	2.628	0.146	1.16248	0.06446	-0.5291	3.2429	0.024	-85.82
242.-249.	50	N2	17.197	0.182	1.21494	0.01285	-1.4790	0.6049	0.870	-30.66
252.-259.	56	M2	90.006	0.181	1.21748	0.00245	-1.8035	0.1155	4.970	-34.75
264.-268.	32	L2	2.779	0.193	1.33002	0.09219	-5.0318	4.0080	0.419	-35.55
270.-273.	16	S2	40.507	0.188	1.17771	0.00545	2.7997	0.2705	2.042	75.71
274.-278.	28	K2	10.930	0.233	1.16870	0.02490	-2.8048	1.2267	0.537	-84.35
315.-3A5.	82	*M3	1.614	0.090	1.12043	0.06280	-6.1243	3.2516	0.182	-71.20

STANDARD DEVIATION D 8.843 SD 7.858 TD 4.013 MICROGAL

QUALITY FACTORS : Q1= 2.2 Q2= 4.3
O1/K1 0.9571 1-O1/1-K1 0.7455 M2/O1 1.0576
CENTRAL EPOCH TJJ= 2442986.5

Table III Wave M2

		4100 Bandung	4103 Babadan		4100 Bandung	4103 Babadan
Observed	A	89.990	88.597	B	5.05	4.30
	δ	1.2173	1.2015	β	-34.3°	-49.2°
	α	-1.81°	-2.11°	$\Delta\overline{B}$	1.42	17°

Oceanic Models

	δ^*	α^*	δ^*	α^*	X	χ	X	χ
SCHW80	*1.1943*	*-0.63°*	*1.1851*	*-0.20°*	*2.69*	*-21°*	*1.69*	*-10°*
CSR 3.0	1.1813	-0.75°	1.1726	0.12°	1.92	-36°	0.76	14°
FES 95.1	1.1848	-0.85°	1.1777	-0.45°	2.22	-35°	1.30	-31°
ORI	1.1870	-1.08°	1.1780	-0.60°	2.56	-40°	1.46	-39°
ORI 96	1.1871	-1.01°	1.1782	-0.53°	2.49	-38°	1.40	-35°
Mean (4)	1.1851		1.1766					

A in μgals, on the basis of the Tamura complete development of the lunisolar potential
α in degrees, a negative phase corresponds to a lag
B vector residue with respect to non hydrostatic, inelastic model inertial correction not applied

Table IV

Wave N2

		4100 Bandung	4103 Babadan	4100 Bandung	4103 Babadan
Observed	A	17.211	17.257	B 0.90	0.97
	δ	1.2159	1.2224	β -29.2°	-30.0°
	α	-1.46°	-1.61°	$\Delta\overline{B}$ 0.05	(82°)

Oceanic Models

	δ^*	α^*	δ^*	α^*	X	χ	X	χ
SCHW80	*1.1845*	*-0.76°*	*1.1928*	*-0.19°*	*0.41*	*-33°*	*0.43*	*-7°*
CSR 3.0	1.1638	-1.64°	1.1651	-0.56°	0.47	-84°	0.16	-77°
FES 95.1	1.1706	-1.56°	1.1775	-0.80°	0.47	-73°	0.31	-48°
ORI	1.1738	-1.55°	1.1787	-0.88°	0.49	-67°	0.34	-48°
ORI 96	1.1754	-1.38°	1.1839	-0.71°	0.45	-62°	0.37	-35°
Mean (4)	1.1709	-1.38°	1.1763	-0.63°				

A in μgals, on the basis of the Tamura complete development of the lunisolar potential
α in degrees, a negative phase corresponds to a lag
B vector residue with respect to non hydrostatic, inelastic model inertial correction not applied

Table V

Wave O1

		4100 Bandung	4103 Babadan	4100 Bandung	4103 Babadan
Observed	A	8.529	9.387	B 1.42	2.00
	δ	1.1530	1.1653	β -85.3°	-86.5°
	α	9.56°	12.28°	$\Delta\bar{B}$ 0.58°	90°

Oceanic Models

	δ^*	α^*	δ^*	α^*	X	χ	X	χ
SCHW80	*1.1930*	*-0.24°*	*1.1808*	*0.69°*	*0.30*	*173°*	*0.25*	*-152°*
CSR 3.0	1.2057	-1.88°	1.1785	-2.00°	0.48	143°	0.38	120°
FES 95.1	1.1801	-0.62°	1.1814	-0.63°	0.22	155°	0.25	155°
ORI	1.1757	-1.76°	1.1510	0.23°	0.31	122°	0.04	(-60°)
ORI 96	1.1796	0.04°	1.1660	0.60°	0.20	182°	0.14	-135°

A in μgals, on the basis of the Tamura complete development of the lunisolar potential
α in degrees, a negative phase corresponds to a lag
B vector residue with respect to non hydrostatic, inelastic model inertial correction not applied

Table VI

Wave S2

		4100 Bandung	4103 Babadan		4100 Bandung	4103 Babadan
Observed	A	40.530	39.702	B	2.18	2.14
	δ	1.1784	1.1573	β	75.2°	-96.3°
	α	2.98°	-3.08°	$\Delta \bar{B}$	4.31	79°

Oceanic Models

	δ^*	α^*	δ^*	α^*	X	χ	X	χ
SCHW80	*1.1903*	*4.02°*	*1.1803*	*-1.80°*	*3.01*	*72°*	*1.40*	*-65°*
CSR 3.0	1.1846	4.35°	1.1852	-1.01°	3.17	77°	1.05	-43°
FES 95.1	1.1826	4.23°	1.1830	-1.73°	3.07	78°	1.40	-61°
ORI	1.1790	4.21°	1.1738	-1.49°	3.06	80°	1.11	-70°
ORI 96	1.1815	4.10°	1.1749	-1.73°	2.97	78°	1.28	-72°
Mean (4)	1.1819	4.22°	1.1792	-1.49°				

A in μgals, on the basis of the Tamura complete development of the lunisolar potential
α in degrees, a negative phase corresponds to a lag
B vector residue with respect to non hydrostatic, inelastic model inertial correction not applied

Table VII

Wave K1

		4100 Bandung	4103 Babadan	4100 Bandung	4103 Babadan
Observed	A	12.453	14.104	B 1.20	3.07
	δ	1.1971	1.2449	β -120.6°	-107.7°
	α	4.77°	11.96°	$\Delta\overline{B}$ 1.92	80°

Oceanic Models

	δ^*	α^*	δ^*	α^*	X	χ	X	χ
SCHW80	*1.1895*	*-4.04°*	*1.1518*	*2.32°*	*1.03*	*122°*	*0.56*	*-108°*
CSR 3.0	1.1856	-7.03°	1.1426	-1.76°	1.57	106°	0.41	101°
FES 95.1	1.2057	-5.66°	1.1640	0.52°	1.41	119°	0.34	-160°
ORI	1.1910	-6.42°	1.1744	0.98°	1.48	111°	0.49	-153°
ORI 96	1.1865	-5.12°	1.1564	0.81°	1.22	114°	0.30	-142°
Mean (5)	1.1917	-5.65°	1.1578	0.57°				

A in μgals, on the basis of the Tamura complete development of the lunisolar potential
α in degrees, a negative phase corresponds to a lag
B vector residue with respect to non hydrostatic, inelastic model inertial correction not applied

TABLE VIII Loading differences Bandung minus Babadan

		ΔB	$\Delta\beta$
M2	$\overline{\Delta B}$	1.42	17°
		ΔL	$\Delta\lambda$
	SCHW80	*1.19*	*65°*
	CSR 3.0	1.81	72°
	FES 95.1	1.22	57°
	ORI	1.27	65°
	ORI96	1.27	65°

		ΔB	$\Delta\beta$
O1		0.58	90°
		ΔL	$\Delta\lambda$
	SCHW80	*0.44*	*80°*
	CSR 3.0	0.65	73°
	FES 95.1	0.59	90°
	ORI	0.33	56°
	ORI96	0.50	79°

		ΔB	$\Delta\beta$
N2	$\overline{\Delta B}$	0.05	82°
		ΔL	$\Delta\lambda$
	SCHW80	*0.21*	*83°*
	CSR 3.0	0.36	100°
	FES 95.1	0.26	87°
	ORI	0.24	94°
	ORI96	0.24	82°

The analysis of the tidal parameters on short measurement intervals

E.A. Boyarsky and L.A. Latynina

Institute of the Physics of the Earth, Russian Academy of Science (IFZ RAN)
Bol.Gruzinskaya, 10, 252810, Moscow, Russia
e-mail: ernst@uipe-ras.scgis.ru
e-mail: lat@uipe-ras.scgis.ru

Abstract. The monitoring of the tidal parameters is attempted at the Protvino observatory with the purpose to discover variations in the physical properties of the environment. The measurements are carried out with four tiltmeters and four strainmeters. According to preliminary analysis of the results, less than 50% of the seasonal amplitude modulation of the waves O_1 and M_2 can be explained by the direct influence of the weather phenomena. The rest possibly relates to the variations sought. This study is mainly methodical in character and aims at future interpretation of the observations at Protvino. Some features of the tidal analysis on short estimation intervals are discussed. In particular, it is shown that the wave interference results in a cycling of errors of the tidal parameter estimates. An outlook of respective software is described as well.

Introduction

Common practice of tidal measurements requires accumulation of maximum possible observations at a station and estimation of the tidal parameters based on this long series. The differences in parameters found in various series at the same station are usually interpreted as a result of measurement errors.
However, there are variations in physical properties of the environment. A greater part of them is induced by weather factors. Firstly, they affect directly the measuring system (gravimeter, tiltmeter, or strainmeter), and in this case we really mean the instrumental errors caused by outer conditions. Secondly, weather factors can bend the terrain surface where tiltmeters are set up. Finally, variations of the temperature, moisture, and water level influence the ground elasticity and, consequently, the tidal parameters. The parameter variations can be a result of the human activity as well.
Provided the effects above have been estimated and eliminated in one way or another, we deal with variations of the ground elasticity that are of the main interest from the viewpoint of their relation to seismicity. Some variations in tidal parameters could serve as short-term (weeks, months) earthquake precursors. Therefore the parameters are to be determined on the same relative short intervals.
There arises a geophysical problem of monitoring the ground elasticity basing on the tidal parameter measurements. The harmonic analysis is not capable to yield these parameters for any specific moment. Therefore it is possible only to determine them on the possible shortest time interval and to connect the results with the middle of this interval. The problem has the following characteristic properties:

- difficulties with wave separation due to the wave mutual interference;
- relatively large influence of measurement errors;
- additional software requirements.

The wave mutual interference

The harmonic analysis allows to separate any two waves if one of them outstrips the other, roughly speaking, by a period during the observations. Otherwise, one has to unite these waves into one wave group and estimate their common parameters (a single amplitude factor and single phase delay). The Moon waves O_1 and M_2 are of the most interest for the monitoring because they are less liable to the insolation. As shown by the experience and model calculations, the parameters of these waves should be estimated on the interval not less 30–40 days.

However, if we can formally separate some wave groups, the shorter estimation interval the worse the least square estimates will correlate. It means that random measurement errors will have a specific influence on several parameters together. If some of them are, for example, underestimated, the others will be regularly either overestimated or also underestimated. The parameter errors are subdued to a strict mathematical relation that includes both the interval length and the phases of all the waves at the beginning of the interval.

Besides, even if errorless measurements were provided, the harmonics would interfere with one another especially on a short estimation interval. We shall exemplify this interference by the effect of the wave S_1 on the estimated O_1 amplitude. The standard theoretical tide at Protvino ($\varphi = 54°.86$, $\lambda = 37°.22$) was used as a basis. Its E—W component with amplitude factor 1.0 was added by the standard wave S_1 (waves 252 and 253 in Cartwright's development) multiplied by 100. As a result, the standard tide has got an extra wave with the period 24 h and the amplitude about 4 milliseconds. We had such amplitude of weather wave at the Protvino observatory in April and May.

With the above model the *ETERNA* program [Wenzel, 1994] gives a rather big deviations of the O_1 amplitude from the theoretical value (Fig. 1). The errors vary in cycles as the estimation interval both increases and slides along time axis. The least errors occur at the interval about 33.7–33.8 days. Especially favourable moments are located approximately every 7.5 days that is obviously associated with "lucky" phase difference for the waves O_1 and S_1. At these moments the error in the O_1 amplitude is minimal, whatever the interval length. Between them there are the most unlucky moments when the error in the O_1 amplitude reaches its maximum. Naturally, the estimate depends on all the other tidal waves, but as the wave S_1 was introduced with factor 100, its influence should be principal. The results would depend on the fact how the waves were grouped, but we follow here H.-G. Wenzel's recommendations. It should be noted, a number of observations always exceeds an estimation interval by the length of the chosen high-frequency filter. Meanwhile, a filter changes the range of estimate fluctuations only by some percents and does not shift the extreme locations.

Now we shall choose one of such unlucky moments (21 of March, 23 h 30 m) and consider how the error depends on the estimation interval length (Fig. 2). The function looks like an attenuated sinusoid. An attenuation is to be expected because there is no interference in estimates on the infinite interval. However, the attenuation is here much slower than we could expect. Evidently, with the given model the error in the O_1 amplitude can not be ignored for observations during a year and more. Even for such long-run measurements the estimate depends in cycles on the estimation interval.

In particular, the cycling in errors means that with the given model the estimate based on 130 days is better than on 138 days. It leads to an intriguing conclusion. Common practice of tidal analysis does not assume that we truncate deliberately the measurements series. However, it could improve the accuracy of the estimates—there is a similar approach in estimation of the mean of oscillations when it is advantageous to keep only an integer number of cycles.

The diurnal meteorological wave S_1 differs inevitably from an ideal sinusoid, and the harmonic analysis interprets this feature as additional waves with multiples of frequencies. The wave S_2 with the period 12h has the biggest influence on the wave M_2. As the standard tide wave S_2 (445th in Cartwright's development) reaches 4.1 milliseconds itself, only double wave S_2 was introduced into the basic model. The waves S_2 and M_2 interference (Fig. 3 and 4) is almost the same as for the waves S_1 and O_1, but much slighter. At the worst, the additional 8 milliseconds of the double wave S_2 distort the estimate of the M_2 amplitude only by 0.1 millisecond (see Fig. 3). In the real measurements at Protvino the whole range of variations in the S_2 amplitude did not exceed 3 milliseconds. Therefore, the observed variations about 1 millisecond in the M_2 amplitude at Protvino can not be explained by interference of the wave S_2.

We have shown the interference of only two pairs of harmonics. A similar study can easily be made for any pair of waves. The interference exists even if waves are in different bands, for instance between S_1 and M_2 which can be separated for sure. It appears that the following steps can be recommended before the harmonic analysis:

- to decide which waves should be estimated with the most accessible accuracy;
- to find out the frequency band where the maximum noise is expected (probably it will be the same notorious wave S_1);

- to synthesise a proper model (a random error can be added if the noise spectrum is known approximately);
- to determine for the model the length of the estimation interval which minimises the error in the wave that we are interested in;
- if necessary, to truncate measurement series.

Generally speaking, location of extremes (Fig. 2 and 4) depends on the amplitude of disturbances, but very weakly. It is quite sufficient to know the amplitudes of the waves S_1 and S_2 with uncertainty about some milliseconds.

Requirements to software

We shall briefly review the software designed in IFZ RAN. A number of geophysical processes are under observation at the Protvino observatory [Latynina et al, 1997]. Readings of four tiltmeters, four strainmeters, barometer, thermometer as well as the water level in a drill hole are recorded every 30 seconds. The preliminary processing mainly consists of the following operations:

- calculation of the GMT moment for each reading (an interval between them slightly differs from the scheduled one due to imperfection of the computer clock and the registration unit);
- replacing of the initial 30 seconds readings by hourly data.

The hourly data are calculated by a direct line or parabola approximation on prescribed time interval, usually ±30 minutes. Simultaneously the readings at the calibration and occasional rough outliers are removed. Measurements can be "cleaned" automatically but it is more reliable to use an effective graph editor included into the preliminary processing program. Later the processing deals only with hourly data.

The tidal analysis on short intervals imposes extra requirements to software. On the one hand, no problem can arise to estimate parameters of long-term waves, with periods of fortnight and more. Hence, it is easy to eliminate a drift with any high-frequency filter. On the other hand, each measurement is more valuable here. There are missing measurements and steps in the reading level, moreover the former ones are often followed by the latter. It would be improper luxury to operate with two or more series on a short estimation interval and to lose their tails while filtering. Therefore, all the measurements should be a single series. It means that we must fill empty places with such calculated values that would not distort the parameter estimates. Besides, we have to determine the moment and the size of each step to correct all the following readings.

We have designed a proper software to solve the above problems. In some cases an iteration process is applied. Thus, if some hourly values are missing and also the reading level has a step, we proceed as follows:

- to take the measurements as separate series, for 20–30 days at each side of the gap;
- to determine the tidal parameters with *ETERNA*;
- to calculate synthetic values for the empty place plus one day before or after;
- to introduce a drift typical for adjacent real data into the calculated values;
- to combine them with the real ones at the overlap zone to move the calculated values to the proper level;
- to insert the calculated values over the empty place;
- to estimate the step size and correct all the following real data.

While the combination of the calculated values with the real readings and estimation of steps is being made, each possible variant of the procedure is tested with the graph editor. In some cases one or two real last readings before a measurement interruption are to be deleted as well. Provided there are no steps, one or two missing readings can easily be inserted in graph editor.

Estimates of steps are more reliable if they are made along the residual curve [Boyarsky et al, 1995]. Student's *t*-criterion and other criteria are used at estimation. Sometimes the moment and size of a step can be measured exactly in the graph editor at preliminary processing, and sometimes only the moment of a step can be determined. For these situations, our software permits to account the known step

correction "by force" and to estimate the step size at the known moment (without the *t*-criterion test of null-hypothesis).
Automation of measurements and the treatment described above have decreased r.m.s. errors of the main Moon waves amplitudes about by a half.
For the harmonic analysis itself, we use the well-known program *ETERNA* ver.2.1 by H.-G. Wenzel. The program was slightly modified, and the user can give the estimation interval length and the step of its moving, both in days or in hours. The program reads initial data only once before all the calculations.

Some preliminary results

An example of the estimates on the sliding interval 34.0 days is in Fig. 5. It shows the results obtained by the pendulum tiltmeter with two-coordinate measuring capacitor [Latynina et al, 1997].
The authors hope to devote a special article to the results after some extra data are accumulated and comprehended. Now we shall briefly touch upon first conclusions. After low frequencies were filtered out and the diurnal and semi-diurnal harmonics were picked up by the *ETERNA* program, r.m.s. residuals occur no more than 1.5 milliseconds in winter but up to 5 milliseconds at the height of summer. This pattern repeats for two years and is the same for both tilt components.
During two intervals (August—November 1997 and April—July 1998) variations in the amplitude estimates are similar. The r.m.s. variation of the M_2 amplitude is 0.2–0.3 milliseconds but it is 0.6–1.3 milliseconds for the wave O_1. These values are, respectively, about 4–5% and 40–50% of their amplitudes. The relative season variations are more 2–3 times.
It would be interesting to determine which part of the observed variations relates to weather phenomena, the air pressure first of all. However the admittance factors calculated on the same four-month series (April—July 1998) are highly controversial. Thus, two tiltmeters allocated on the common basement and oriented in the same N—S direction had significantly different admittances: -0.081 ± 0.006 and -0.046 ± 0.006 milliseconds/hPa. Up to the present, there is the only one, rather disputable, explanation that the cast iron basement plate has sagged. After the proper correction of the tiltmeter readings, the amplitude estimates changed barely by 0.01–0.02 milliseconds for the wave M_2 and 0.2–0.3 milliseconds for O_1. Both these changes are several times less than the variations of amplitude. Thus, if the atmospheric pressure affects the tiltmeter readings it does it neither directly nor instantly. Besides, the admittance can depend on frequency band as it was shown for example by Polzer et al [1996], Kroner and Jentzsch [1998], and Onoue and Takemoto [1998]. The tilt and strain are influenced by the atmospheric pressure less than the gravity. This effect should depend most probably on horizontal gradient of air pressure and local topography. Therefore, one can hope that a local admittance factor would be sufficient to reduce measurements with a tiltmeter and strainmeter.
Similar corrections, accounting for the water level in the drill hole, changed the amplitude estimates for the waves M_2 and O_1 even less. Although variation in the water level has a diurnal harmonic determined obviously by the life and work of local population that is clear from comparison of variations on working days and weekends (Fig. 6).

Conclusions

The wave M_2 amplitude varies by some percents during a year, and the wave O_1 amplitude up to 100%. The diurnal variations of the atmospheric pressure and of the water table (as well as their non-sinusoidal form) distort the tidal waves. However, the effect of the weather wave S_1 and its multiple frequencies can explain only a smaller part of variations of those waves during the period of our study.
This study is a stage of creating a method to discover earthquake precursors that have a tidal origin. The specificity of the tidal analysis restricts the study area to short-term (weeks, months) and middle-term (years) precursors. For processes that last some months, we have to analyse the tidal waves on the optimal estimation interval 34 days. The Moon waves of the most reliable determination are taken for

study purposes, but even those waves are affected by weather variations. Therefore, the tidal parameters estimated on a short measurement series inevitably include a meteorological component.
The diurnal weather variations in the temperature and other factors should affect the results of the tidal analysis for long-run measurements as well, as their influence is not compensated perfectly over a year. The weather conditions themselves vary from year to year; there are also quasi-periodical climate cycles. These factors impose a great noise level into tidal monitoring of seismotectonic processes.

The study was supported by grants EC Copernicus ERBIC15CT960205 and RFFI 98–05–64761.

References

Boyarsky E.A., Volkov V.A., Afanasieva L.V., 1995

Боярский Э.А., Волков В.А., Афанасьева Л.В.
Преимущества обработки земноприливных наблюдений по остаточной кривой.
Физика Земли, 1995, 11, с. 68–73

Kroner C. and Jentzsch G., Comparison of Air Pressure Reducing Methods and Discussion of Other Influences on Gravity. Proc. of the XIII Int. Symposium on Earth Tides. Brussels, 1998, 423–430.

Latynina L.A., Boyarsky E.A., Vasiliev I.M., Sorokin V.L, 1997

Латынина Л.А., Боярский Э.А., Васильев И.М., Сорокин В.Л.
Наклономерные наблюдения на подмосковной станции Протвино.
Физика Земли, 1997, 11, с. 86–93

Onoue K. and Takemoto S., Atmospheric Pressure Effect on Ground Strain Observation at Donzurubo Observatory, Nara, Japan, Proc. of the XIII Int. Symposium on Earth Tides. Brussels, 1998, 157–164.

Polzer G., Zürn W., Wenzel, H.–G. , 1996. NDFW Analysis of Gravity, Strain and Tilt Data from BFO., Bull. Inf. Marées Terrestres, 125: 9514–9545.

Wenzel, H.–G. , 1994. Earth Tide Data Processing Package. Bull. Inf. Marées Terrestres, 120: 9019–9021.

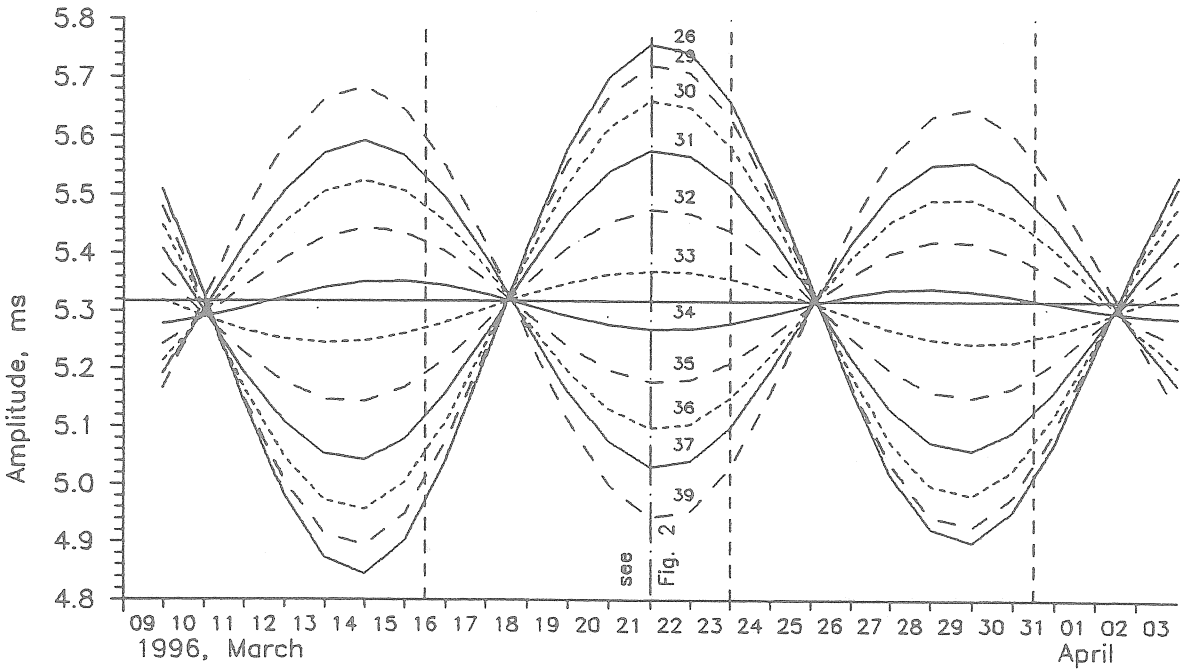

Fig. 1: The wave O1 amplitude vs the middle of estimation interval for its various lengths (indicated in days). The vertical lines are spaced 7.50 days. The horisontal line is the theory value 5.317 ms.

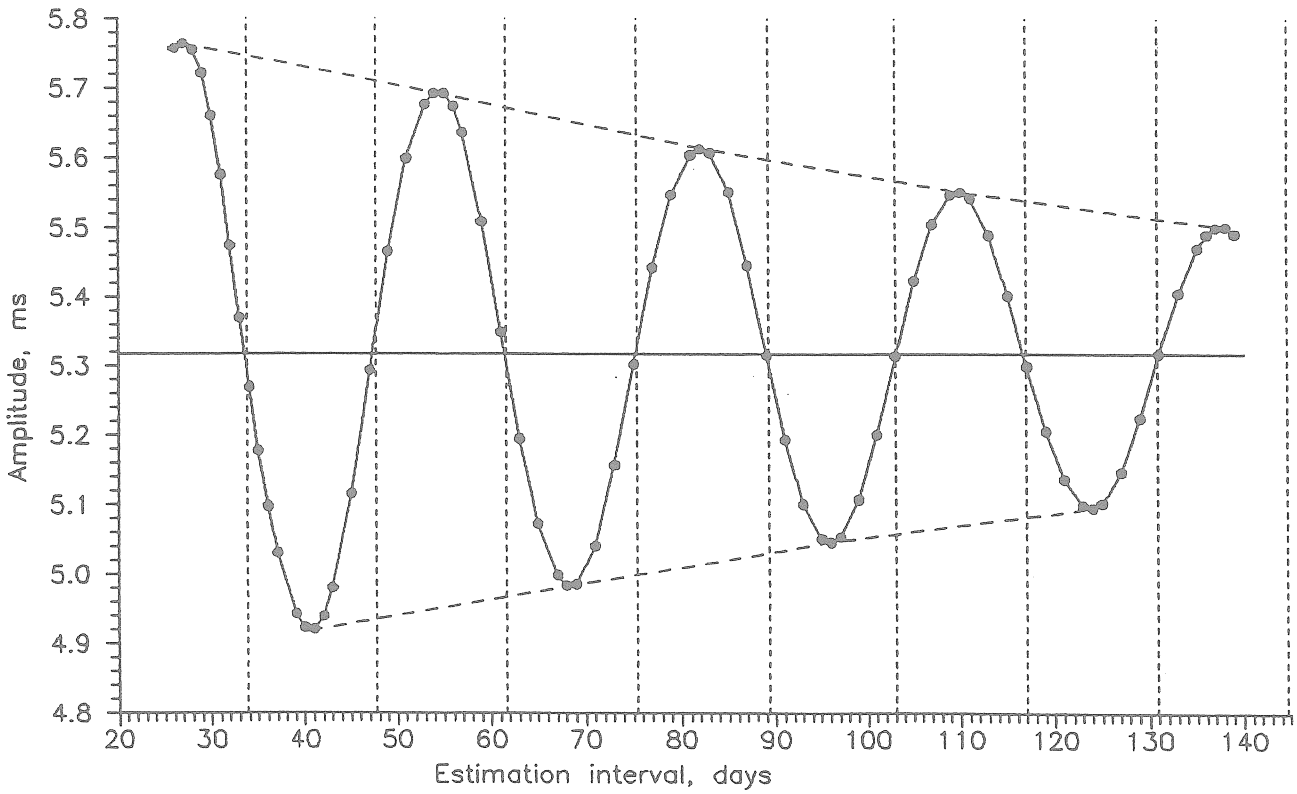

Fig. 2: The wave O1 amplitude vs estimation interval length at 21 of March, 23h 30m. The vertical lines are spaced 13.85 days.

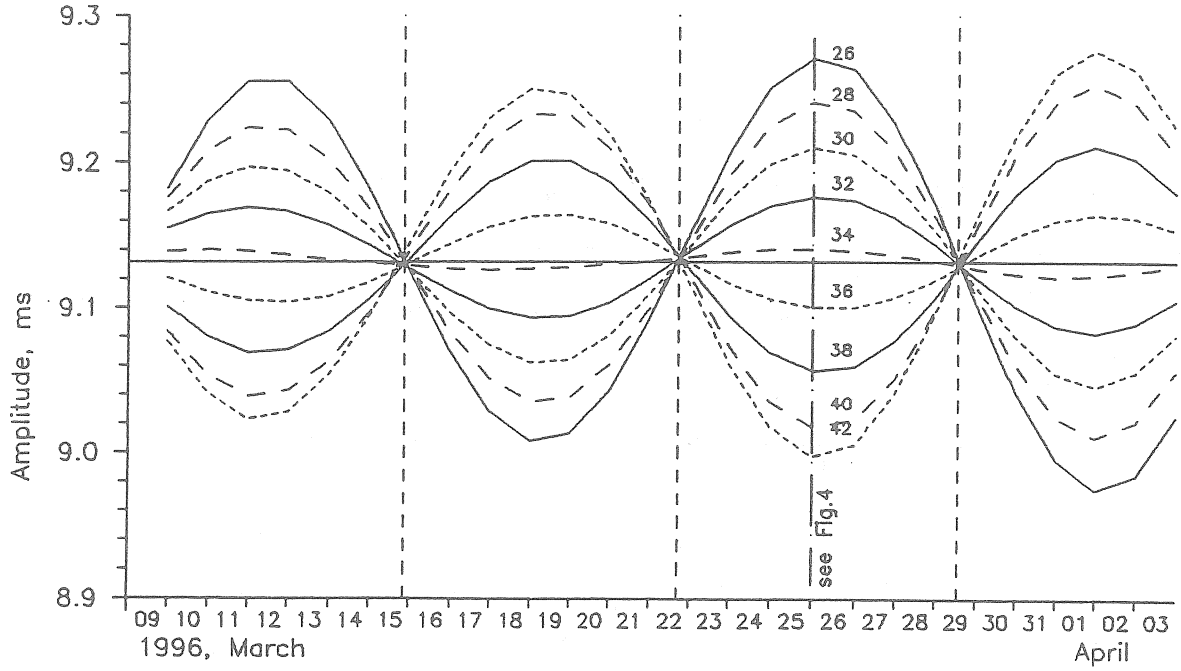

Fig. 3: The wave M2 amplitude vs the middle of estimation interval for its various lengths (indicated in days). The vertical lines are spaced 6.85 days. The horisontal line is the theory value 9.132 ms.

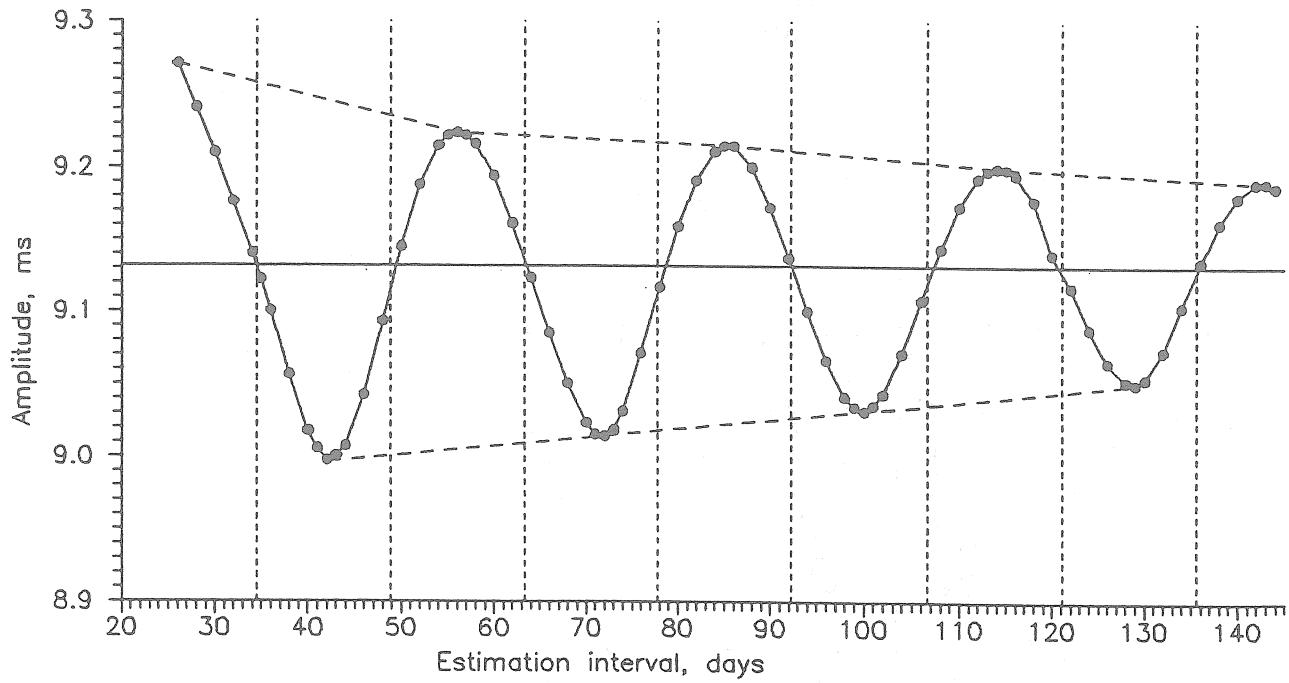

Fig. 4: The wave M2 amplitude vs estimation interval length at 25 of March, 23h 30m. The vertical lines are spaced 14.45 days.

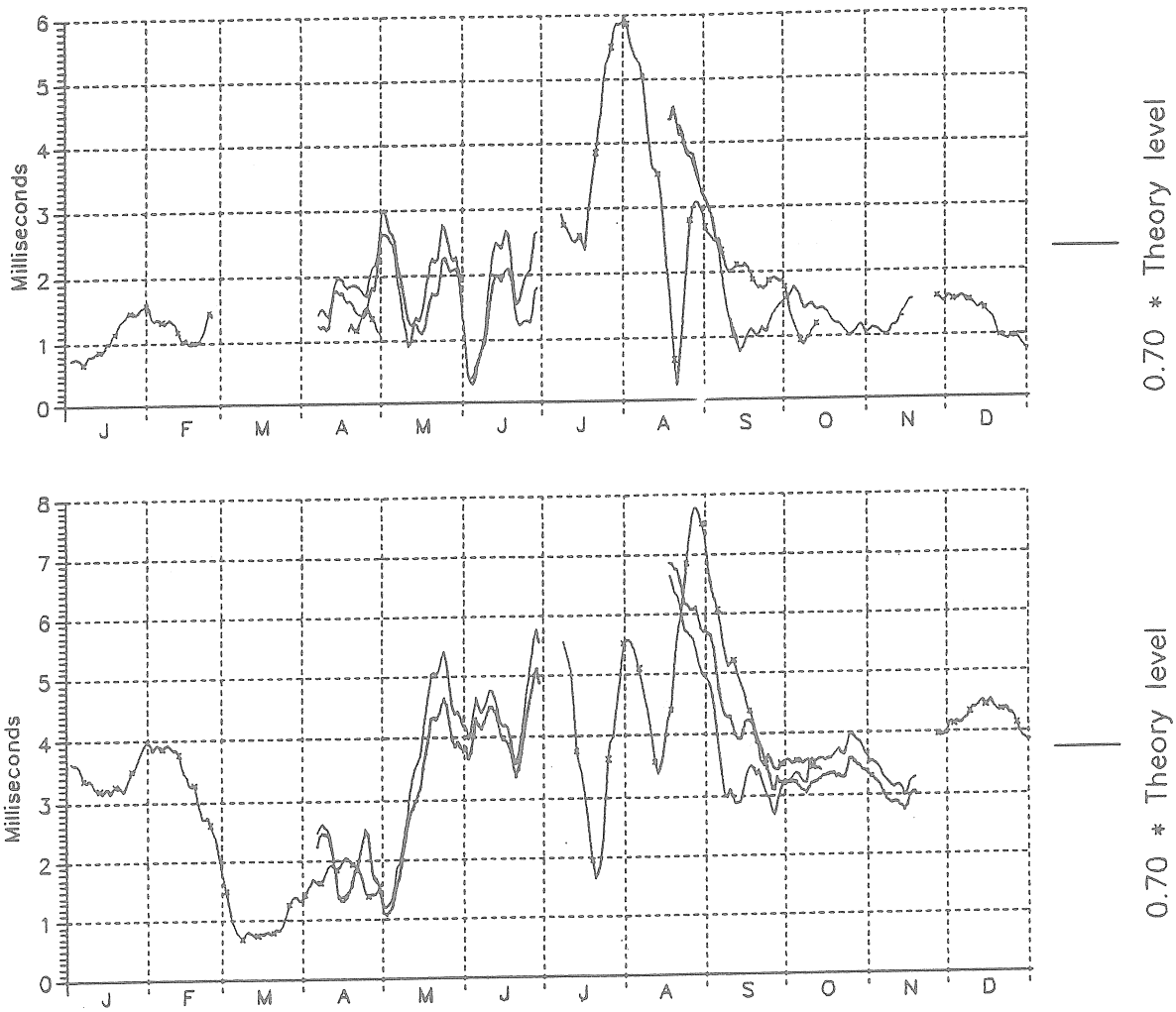

Fig. 5: Amplitudes of the waves O1 in Protvino.
N–S (above), E–W (below)

1995–1996
1997–1998

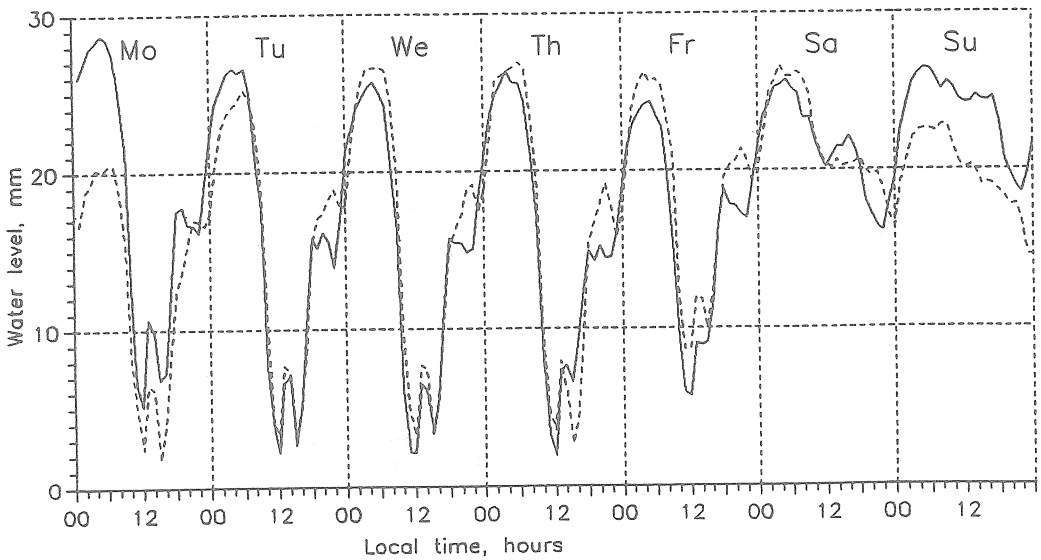

Fig. 6: Variations of water level in the drill hole averaged over a week

1997, September – November
1998, April – June

Traduction

PERTURBATIONS IRREGULIERES DE LA DERIVE D'UN EXTENSOMETRE VERTICAL EN RELATION AVEC LES VARIATIONS DE LA PRESSION ATMOSPHERIQUE

R.M. Uruchadse

Communications de l'Académie des Sciences de Géorgie
135, n° 2, pp 93-96, 1989

Les forces génératrices de marées luni-solaires perturbent en permanence le champ de gravitation de la Terre tandis que la Terre elle-même à cause de sa dimension propre subit des déformations périodiques.

Dans la théorie statique des marées terrestres tous les phénomènes provoqués par les forces génératrices de marées peuvent être caractérisés par les nombres h, k, et f: h et k sont introduits par Love; est le nombre de Shida et f porte le nom de quatrième nombre de Love: il établit le lien entre la dilatation cubique de la matière terrestre et le potentiel de la force génératrice de marées et il peut être déterminé à l'aide d'un extensomètre vertical [1].

La haute sensibilité de l'appareil enregistreur de marées et également la possibilité d'enregistrer les processus de déformation dans un large diapason de périodes (depuis quelques secondes jusqu'à un an) déterminent la suprématie de la méthode donnée lors de l'étude de l'écorce terrestre en comparaison avec les autres méthodes.

Avec l'augmentation de la sensibilité et de la qualité des observations des appareils enregistreurs de marées et également avec le développement des méthodes de réduction mathématique sont apparus des problèmes en relation avec le fait que toutes les observations de marées terrestres sont perturbées par des effets répétitifs liés aux facteurs météorologiques et aux conditions locales provoquées par les variations de température et de la pression atmosphérique. Ils produisent une déformation de la surface de la Terre dont l'amplitude peut être importante.

Le calcul des facteurs météorologiques est compliqué puisqu'ils influencent aussi bien les installations de mesure que le sol. La pression peut varier de 10mb et plus au cours du jour et, lors du passage des cyclones et des anticyclones, les chutes de pression atteignent 20 à 30 mb ce qui conduit à l'enregistrement de déformations apparentes comparables avec les marées. On n'a plus à présent aucun doute que la variation de la pression atmosphérique exerce une influence sur les résultats des observations clinométriques, extensométriques et gravimétriques [2] ce qui résulte des déformations régionales de la surface de la Terre et des blocs séparés de l'écorce terrestre [3].

Il convient de noter que les questions de l'influence perturbatrice des variations de la pression atmosphérique sur les observations de marées ont été insuffisamment prises en considération jusqu'à ce jour. Pour étudier l'influence perturbatrice de la variation de la pression atmosphérique sur les indi-

cations d'un extensomètre vertical il faut disposer des données de mesure de la pression atmosphérique aussi bien au point des observations de marées qu'au minimum dans deux directions (NS et EW) à une distance de quelques centaines de kilomètres. Ces données doivent être continues et synchronisées avec les observations de marées.

Dans la Section des Marées Terrestres de l'Institut de géophysique de l'Académie des Sciences de Géorgie on a organisé en 1984, en simultanéité avec les observations de l'extensomètre vertical, des observations continues de haute précision des variations de la pression atmosphérique pour que soit préparé un appareil de mesure photoélectrique de la pression sur la base du météorographe H-22. L'enregistrement a été fait à l'aide de l'enregistreur du type KCπ-4 avec l'échelle (- 10 mb - à + 10 mb). L'échelle de la pression atmosphérique peut atteindre 10^{-3} mb/mm.

Disposant des données de la variation de la pression atmosphérique et des données de l'extensomètre vertical nous avons comparé la dérive de l'extensomètre vertical à l'évolution de la pression atmosphérique (figure 1) pour un intervalle de temps d'une durée de 3600 h. Une corrélation particulièrement bonne s'observe sur les parties des courbes a - b, a' - b'.

On a déterminé le coefficient barométrique de l'extensomètre vertical dont la valeur numérique détermine la variation de l'indication de l'extensomètre vertical en unités relatives des déformations, correspondant à la variation de la pression atmosphérique en mb. Les résultats de la détermination du coefficient barométrique de l'extensomètre vertical sont donnés dans la table où l'on constate qu'à un accroissement de la pression atmosphérique correspond une diminution à la base de l'extensomètre vertical. Pour notre extensomètre la valeur du coefficient barométrique était

$$\beta = \Delta p/\Delta y \ (4.98 \pm 0.67) \ 10^{-9}/ \text{ mb}.$$

On a effectué une estimation de l'influence des variations diurnes et semi-diurnes de la pression atmosphérique sur les paramètres des ondes de marées M_2, N_2, K_1 et O_1. Il est apparu clairement que l'influence directe des variations de la pression atmosphérique sur les appareils enregistreurs de marées agit peu sur les valeurs indiquées des paramètres de marées. Le contraire est observé pour l'onde S_2. Cela s'explique par le fait que pour cette onde aussi bien l'amplitude que la différence de phase avec l'onde analogue dans la marée élastique de la Terre se conservent invariables sur la durée d'un an.

L'analyse des données a montré que les variations de la pression atmosphérique perturbent sensiblement uniquement les constantes harmoniques des ondes de marées K_2, S_2, P_1, M_1, S_1. Pour une estimation de qualité de l'influence de la variation de la pression atmosphérique sur les paramètres des différentes ondes de marées on a fait une analyse spectrale d'une série d'observations de l'extensomètre vertical et du barographe photoélectrique d'une durée commune de 1024 h. On a calculé les spectres de densité à l'aide de la transformation rapide de Fourier. Nous donnons sur la figure 2 les résultats de ces calculs.
On constate qu'une influence particulièrement forte sur les enregistrements de l'extensomètre vertical produit une composante de basse fréquence (10^{-4} - 10^{-6} hertz) de la pression atmosphérique.
Les données permettent de conclure que lors d'observations de longue durée des marées à l'aide d'un appareil extensométrique mais également gravimétrique et

clinométrique il est nécessaire de faire une étude des variations de la pression atmosphérique pour introduire les corrections correspondantes.

Références

1. Б. К. Балавадзе, К. З. Картвелишвили, Р. М. Урушадзе. Сообщения АН ГССР, 129, № 3, 1988, 541.
2. Б. К. Балавадзе, К. З. Картвелишвили. Приливы в твердом теле Земли. Тбилиси, 1984.
3. P. Melchior. The Tides of the Planet Earth. Pergamon Press, 1978.

Table 1 Détermination du coefficient barométrique pour l'extensomètre vertical $\beta = \Delta p/\Delta y$ (10^{-9})

	Date de la détermination	Différence de pression (mm. enreg)	Différence de dérive (mm. enreg.)	Coefficient
1	18.3 - 23.3.1984	26	250	3,425
2	24.3 - 29.3 "	32	310	3,451
3	1.4 - 4.4 "	14	130	3,306
4	4.4 - 6.4 "	14	170	4,323
5	1.9 - 5.9 "	9	104	4,114
6	5.9 - 8.9 "	17	100	4,559
7	18.9 - 22.9 "	15	180	9,300
8	22.9 - 23.9 "	17	44	4,305
9	1.11 - 2.11 "	9	50	4,011
10	3.11 - 4.11 "	9	104	8,955
	Moyenne			4,98
	Erreur moyenne arithmétique			1,66
	Erreur quadratique moyenne			0,67

clinométrique il est nécessaire de faire une étude des variations de la pression atmosphérique pour introduire les corrections correspondantes.

Références

1. Б. К. Балавадзе, К. З. Картвелишвили, Р. М. Урушадзе. Сообщения АН ГССР, 129, № 3, 1988, 541.
2. Б. К. Балавадзе, К. З. Картвелишвили. Приливы в твердом теле Земли. Тбилиси, 1984.
3. P. Melchior. The Tides of the Planet Earth. Pergamon Press, 1978.

Table 1 Détermination du coefficient barométrique pour l'extensomètre vertical $\beta = \Delta p/\Delta y$ (10^{-9})

	Date de la détermination	Différence de pression (mm. enreg)	Différence de dérive (mm. enreg.)	Coefficient
1	18.3 - 23.3.1984	26	250	3,425
2	24.3 - 29.3 "	32	310	3,451
3	1.4 - 4.4 "	14	130	3,306
4	4.4 - 6.4 "	14	170	4,323
5	1.9 - 5.9 "	9	104	4,114
6	5.9 - 8.9 "	17	100	4,559
7	18.9 - 22.9 "	15	180	9,300
8	22.9 - 23.9 "	17	44	4,305
9	1.11 - 2.11 "	9	50	4,011
10	3.11 - 4.11 "	9	104	8,955
	Moyenne			4,98
	Erreur moyenne arithmétique			1,66
	Erreur quadratique moyenne			0,67

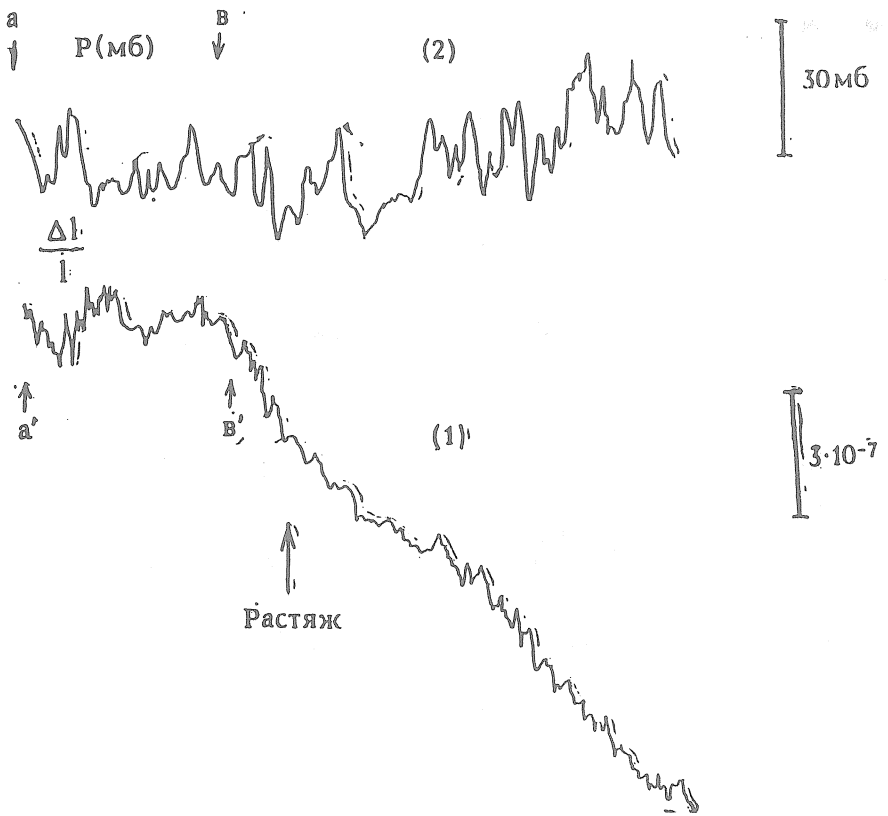

Figure 1 Dérive de l'extensomètre vertical et évolution de la variation moyenne semi-diurne de la pression atmosphérique: 1 - dérive de l'extensomètre, 2 - évolution de la variation moyenne diurne de la pression atmosphérique.

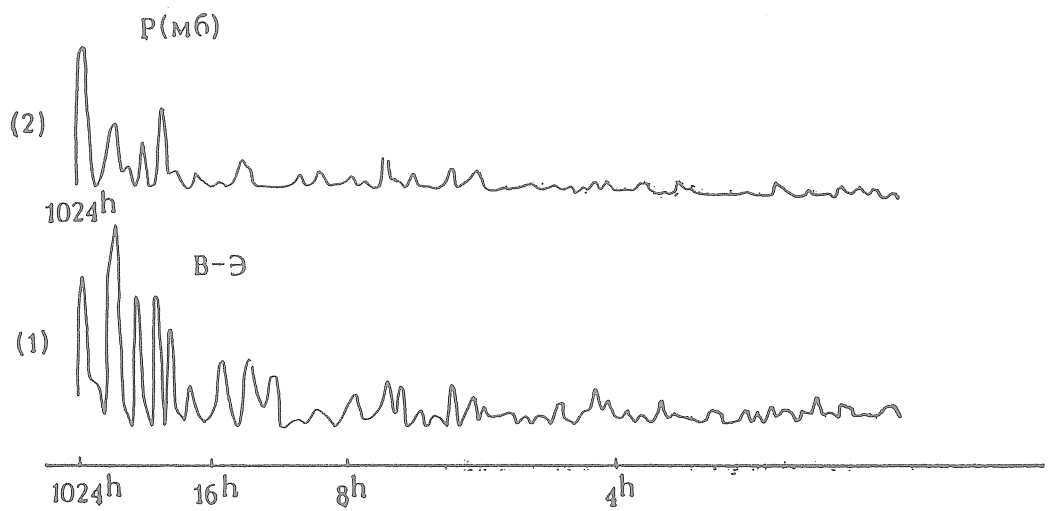

Figure 2 Spectre d'amplitude de l'enregistrement de 1024 heures; 1 de l'extensomètre vertical, 2 du barographe.

Observations of the Earth tide vertical extensions in the old Osakayama tunnel.

By Izuo OZAWA
Geophysical Institute, Kyoto University

1. Observation in well, V5.
2. Observation on vertical diameter of cross-section of tunnel, V3.
3. Topographical effect.

Abstract

Observations of the Earth tide vertical extension, V_5 have been performed using an extensometer set in a well in the old Osakayama tunnel from 1963 to 1985. The 55.026 observed hourly values are analysed for the 8 principal tidal waves. For the M_2 wave the effect of the oceanic load tide is subtracted and the direct effect is obtained as

$$M_2 = 0.464 \times 10^{-8} \cos (2t - 185.86°)$$

Given the Love number $h_2 = 0.60$ and the theoretical tide generating potential, W_2, one obtains $(a\partial h_2 / \partial r)_{r=a} = - 1.38$, where r and a are the radius vector from the Earth's centre and the mean radius of the Earth respectively.
The phase lags of M_2, O_1 and S_2 are 185.36°, 197.04° and 154.23°, respectively.
The reason for the difference between the phase lags of O_1 and M_2 is not clear. But the difference between S_2 and M_2 seems to be due to the effects of the atmospheric tide and solar heat radiation. The semi-diurnal component of the solar heat radiation is obtained.

The tidal contraction of the vertical diameter of the cross-section of the tunnel, V_3 has been estimated for the period of 1963 - 1984. One expects that the contraction is amplified by cavity effect, such that the expected contraction will be about 4 times the contraction observed at a long distance from the tunnel. 20,929 hourly observed values are analysed. The comparison between V_5 and V_3, gives an amplitude ratio, $V_3/V_5 = 3.09$ and a phase difference, $V_3 - V_5 = 2.7°$.

1. Observations of the vertical extension, V5, in a well

1. Observations of tidal extensions have been performed in a well in the old Osakayama tunnel (34°59'N. lat., 135°54'E. long.) from 1963 to 1985. In order to prevent the ground subsidence caused by digging the well, the outside of the pipe in which the extensometer, V5, is set, is densely filled with rock pieces.
A harmonic analysis has been performed on 55,062 hourly data divided into 33 series between 1963 and 1985 to obtain the 8 waves, M_2, O_1, S_1, S_2, K_1, K_2, P_1 and N_2. Table 1 shows the amplitudes and phase lags of the waves M_2, O_1, and S_2

Table 1. Amplitudes and phase lags of M_2, O_1, and S_2 waves of the vertical extension in well in old Osakayama tunnel.

Epoch	Analyzed hours	M_2-wave Amplitude $\times 10^{-8}$	M_2-wave Phase	O_1-wave Amplitude $\times 10^{-8}$	O_1-wave Phase	S_2-wave Amplitude $\times 10^{-8}$	S_2-wave Phase
1964 Aug.11	718	0.641	119.69°	0.341	213.10°	0.265	171.21°
1964 Sep.15	705	0.625	206.20	0.397	211.23	0.361	103.45
1964 Oct.15	1291	0.686	180.18	0.391	210.75	0.313	148.45
1965 Jan.13	1013	0.736	188.47	0.426	193.36	0.240	147.18
1965 Mar. 8	1678	0.659	189.80	0.310	187.12	0.560	137.59
1965 Oct. 1	603	0.669	184.75	0.351	191.17	0.299	159.50
1965 Nov. 4	772	0.546	188.65	0.346	197.73	0.163	148.44
1966 Feb.28	970	0.418	180.08	0.267	195.98	0.227	164.79
1966 Aug.27	1500	0.485	172.51	0.333	187.75	0.262	178.49
1967 May 4	1524	0.426	176.16	0.305	192.14	0.143	121.71
1967 Sep.12	2164	0.598	180.78	0.413	189.23	0.344	118.60
1968 Sep.21	1944	0.566	196.13	0.511	218.21	0.248	147.18
1970 Jan.24	5643	0.450	196.84	0.292	203.94	0.248	147.18
1970 Sep.17	4463	0.666	181.68	0.488	197.42	0.180	147.21
1971 Mar.19	2205	0.323	193.18	0.200	189.25	0.116	101.90
1971 Sep.12	3173	0.373	181.02	0.232	194.93	0.125	172.53
1972 Feb.12	2916	0.386	176.84	0.244	191.13	0.174	156.38
1972 Jul.21	1380	0.379	182.54	0.227	180.66	0.176	196.22
1980 Jan. 8	1523	0.456	179.60	0.145	192.70	0.147	175.68
1980 Mar.10	1673	0.479	185.83	0.169	199.22	0.226	159.93
1980 May 20	1261	0.452	182.72	0.173	191.37	0.135	170.64
1980 Sep.16	792	0.387	190.82	0.182	197.79	0.167	176.04
1980 Oct.17	791	0.393	197.36	0.182	207.75	0.216	161.20
1980 Nov.16	1123	0.462	193.59	0.182	192.04	0.143	160.02
1980 Dec.30	1238	0.468	190.88	0.276	196.68	0.150	189.04
1981 Feb.17	1857	0.411	173.18	0.142	187.02	0.212	163.36
1981 May 4	3179	0.353	187.42	0.127	193.03	0.143	196.77
1981 Nov. 4	1309	0.729	188.30	0.300	202.14	0.310	168.72
1982 Sep.10	1598	0.683	179.90	0.367	191.49	0.312	165.75
1982 Dec.14	1956	0.635	187.55	0.332	193.76	0.112	172.62
1983 Mar. 5	1164	0.642	190.06	0.353	189.86	0.268	144.75
1984 Dec.31	1806	0.403	185.95	0.269	201.84	0.114	168.68
1985 May 9	939	0.594	194.54	0.286	193.74	0.220	120.63

The mean values of the 8 component-waves are obtained tentatively as follows,

$$M_2 = 0.483\times10^{-8}\cos(2t-185.36°), \quad \text{.....(I-1)}$$
$$O_1 = 0.285\times10^{-8}\cos(t-197.04°), \quad \text{.....(I-2)}$$
$$S_1 = 0.056\times10^{-8}\cos(t-198.53°), \quad \text{.....(I-3)}$$
$$S_2 = 0.183\times10^{-8}\cos(2t-154.23°), \quad \text{.....(I-4)}$$
$$K_1 = 0.123\times10^{-8}\cos(t-222.29°), \quad \text{.....(I-5)}$$
$$K_2 = 0.145\times10^{-8}\cos(2t-174.72°), \quad \text{.....(I-6)}$$
$$P_1 = 0.074\times10^{-8}\cos(t-221.78°), \quad \text{.....(I-7)}$$
$$N_2 = 0.118\times10^{-8}\cos(2t-178.87°). \quad \text{.....(I-8)}$$

The phase of O_1 lags that of M_2 by 11.68°. We do not know the cause of this lag but we speculate that the M_2 wave is a semi-diurnal tide while O_1 wave is a diurnal tide. The phase of S_2 is 31.13° in advance of M_2 because S_2 wave is affected by the atmospheric pressure tide and the solar heat radiation. The most important indirect effect is the load tide caused by the oceanic tide. But, in the vertical extension, the load tide is much smaller than in horizontal extensions. Suppose that the Earth is covered with sea-regions of constant height tide. The relative strain components, $e'_{\theta\theta}$, $e'_{\lambda\lambda}$, and e_r' caused by the load tide on the sea region which is surrounded with 1° distant angle and 1° azimuth angle of great circles at the distance of θ° are given in the Table 2. We can see that e_r' is smaller than one tenth of $e'_{\theta\theta}$, and $e'_{\lambda\lambda}$, within the distant angle 6°. These effects rapidly decrease with θ. If the Earth is totally covered with a constant high tide, $\Sigma e_r'$ is smaller by a factor $-0.027\ \Sigma e'_{\theta\theta}$, and $0.034\ \Sigma e'_{\lambda\lambda}$. Green's functions (Farrell, 1972 Table A4) show $e_r' = -0.334\ (e'_{\theta\theta} + e'_{\lambda\lambda})$ on the oceanic mantle. And also $e'_{\theta\theta} \times e'_{\lambda\lambda} < 0$ in the almost sea-regions. Consequently, as in the load tide, the vertical extension is much smaller than the horizontal extensions and the direct effect of the vertical extension is correctly obtained.

Σ e' are the relative values of the oceanic load tide when the entire Earth is covered with a unit height tide.
Using the tidal charts by H. Nishida (1980) and S. Ogura (1933) that describe the tide in the regions limited by the longitudes 110° E and 160° E and the latitudes 0° and 60° N, we obtain the M_2 wave load in the vertical extension :

$$0.0192 \times 10^{-8} \cos (2t - 176.72°) \qquad \text{(II - 1)}$$

Using the Schwiderski map (1980) which gives the M_2 wave outside the region of Nishida and Ogura charts, the vertical extension caused by the loading is

$$0.0012 \times 10^{-8} \cos (2t - 118°) \qquad \text{(II - 2)}$$

Subtracting these calculated load tides of the extension (II - 1) and (II - 2) from the observed value, (I - 1), one obtains the direct effect :

$$0.464 \times 10^{-8} \cos (2t - 185.86°) \qquad \text{(III)}$$

The relationship between the Earth tide direct effect of the vertical extension, e_r and the tide generating potential of the second degree, W_2, is given as

$$e_r = (a\, \partial h_2 / \partial r + 2h_2)\, W_2 / ag, \qquad (1)$$

where a, h_2, r and g are the mean radius of the Earth, the Love number, the radius vector from the centre and the gravitational acceleration at the Earth's surface, respectively.
From (III) and equation (1), and supposing $h_2 = 0.60$, we have

$$a\, \partial h_2 / \partial r = -1.38 \qquad \text{(IV)}$$

Table 2. Relative values of strain components of oceanic load tide, $e'_{\theta\theta}$, $e'_{\lambda\lambda}$ and e_{π}' due to unit loading on sea area of angular distant 1° x azimuth distant 1° surrounded the great circle at angular distant θ.

θ	$e\theta\theta'$	$e\lambda\lambda'$	$e_{,,}'$
1°	431.065	-355.560	1.014
2	203.760	-152.363	-17.017
6	32.837	-25.127	-2.553
10	8.465	-12.548	1.352
20	1.999	-6.297	1.423
30	2.013	-3.464	0.480
40	2.690	-1.284	-0.465
50	2.945	0.308	-1.077
60	2.569	1.230	-1.258
70	1.781	1.540	-1.110
80	0.904	1.412	-0.767
90	0.160	1.064	-0.399
100	-0.345	0.608	-0.084
110	-0.631	0.210	0.139
120	-0.722	-0.093	0.270
130	-0.814	-0.278	0.362
140	-0.589	-0.359	0.314
150	-0.452	-0.345	0.264
160	-0.299	-0.265	0.187
170	-0.147	-0.143	0.096
180	0	0	0
Σ e'	686.97	-551.75	-18.83

Causes of phase advance of S_2

Since the oceanic load tide is very small for the vertical extension, the sum of the direct effect and the oceanic load tide is calculated using the observed value of M_2 wave (I - 1) and the coefficient ratio, $S_2 / M_2 = 0.46$ of the tide generating potential as follows,

$$e_{\pi}(S_2) = 0.225 \times 10^{-8} \cos(2t - 185.86°) \qquad (V)$$

Subtracting the above expression, (V) from observed value of S_2 (I - 4) gives the sum of the atmospheric load tide and the effect of the solar heat radiation. The result is

$$e_{\pi}''(S_2) = 0.117 \times 10^{-8} \cos(2t - 59.18°) \qquad (VI)$$

The atmospheric load tide has been calculated by Ozawa (1984, 1986) as

$$0.0667 \times 10^{-8} \cos(2t - 341.73°) \qquad (VII)$$

From (VI) and (VII) the effect of the solar radiation is

$$0.121 \times 10^{-8} \cos(2t - 91.61°) \qquad (VIII)$$

2. Observations of the tidal extension on the vertical diameter of the cross-section of the tunnel

The observation of extension along the vertical borehole is the ideal method to observe the Earth tide vertical component. This method, however, is not convenient to monitor the behaviour of the instrument in the hole. There are short period disturbances, shorter than 1 hour, in ground water pressure in the observations. Conversely, there are few disturbances on the observations on the extension of the vertical diameter of the cross-section of the tunnel. In this case it is easy to also monitor the behaviour of the instrument, and to maintain high sensitive observations.

The extension of the diameter caused by a horizontal tension in the radial direction is amplified 3 times for the horizontal component of a circular hole, and 4 times for the vertical component by the cavity effect. This amplification is very useful for observations of minute variations caused by the Earth tide.

Fig. 1 shows registrations of the vertical contraction, V5, in the well and that of V3, on the vertical diameter of the cross-section of the tunnel.
Photo 1(a) and (b) show the observing records of the vertical contraction, V5, in the well and that of V3, on the vertical diameter of the cross-setion of the tunnel, respectively.
Table 3 gives the amplitudes and the phase lags of M_2, O_1 and S_2 waves of the vertical extension of V3 (20,929 hours analysed in 22 series between 1694 and 1982).

Table 3. The amplitudes and phase lags of M_2, O_1 and S_2 of the vertical extension on the vertical diameter on cross-section of old Osakayama tunnel.

Epoch	Analyzed hours	M_2		O_1		S_2	
		Amplitude $\times 10^{-8}$	Phase	Amplitude $\times 10^{-8}$	Phase	Amplitude $\times 10^{-8}$	Phase
1964 Jan.06,	665	1.745	172.22°	0.760	185.52°	1.835	148.43°
1964 Feb.15,	1308	1.405	178.69	0.560	243.24	0.845	150.22
1964 Apr.14,	900	1.400	204.03	0.825	213.68	1.070	127.86
1964 May 26,	770	1.270	201.70	0.385	227.84	0.525	136.06
1964 Jun.03,	2572	1.665	214.16	0.895	254.30	1.035	141.19
1964 Oct.23,	988	1.840	204.48	0.647	212.37	0.587	111.21
1979 Dec.18,	840	1.613	180.18	0.572	199.74	0.849	109.95
1980 Feb.02,	876	1.470	152.45	0.518	179.38	0.738	130.17
1980 Apr.15,	722	1.662	185.98	0.481	217.72	1.254	137.53
1980 May 20,	998	1.645	181.01	0.638	200.46	1.011	130.45
1980 Jul.08,	99	2.769	202.52	1.581	273.22	2.579	138.68
1980 Jul.15,	223	1.111	181.10	0.461	195.74	0.488	54.70
1980 Jul.29,	459	1.445	174.75	0.545	202.23	0.684	162.32
1980 Aug.26,	120	1.665	184.84	1.595	78.09	1.556	69.32
1980 Sep.03,	314	1.468	181.99	0.979	211.06	1.279	146.60
1980 Nov.11,	280	1.837	175.96	0.188	191.02	1.080	99.67
1980 Dec.16,	1500	1.579	186.27	0.609	202.00	0.750	136.19
1981 Feb.15,	1003	1.545	183.56	0.695	190.61	0.949	161.46
1981 Apr.14,	1512	1.579	184.61	0.427	189.39	0.977	133.21
1981 Jun.15,	1584	1.500	180.29	0.675	186.08	0.872	144.81
1981 Aug.25,	1068	1.439	184.22	0.586	184.55	0.902	147.74
1981 Oct.13,	1995	1.549	184.22	0.639	187.52	0.786	143.64

The mean values for the 8 main waves of the vertical extension are tentatively calculated as follows,

M_2 : $1.494 \times 10^{-8} \cos(2t - 188.10°)$, (IX - 1)
O_1 : $0.565 \times 10^{-8} \cos(t - 208.88°)$, (IX - 2)
S_1 : $0.232 \times 10^{-8} \cos(t - 68.34°)$, (IX.- 3)
S_2 : $0.866 \times 10^{-8} \cos(2t - 139.17°)$, (IX - 4)
K_1 : $0.210 \times 10^{-8} \cos(t - 208.35°)$, (IX - 5)
K_2 : $0.268 \times 10^{-8} \cos(2t - 3.12°)$, (IX - 6)
P_1 : $0.375 \times 10^{-8} \cos(t - 171.61°)$, (IX - 7)
N_2 : $0.158 \times 10^{-8} \cos(2t - 180.30°)$, (IX - 8)

The amplitude ratio, V3/V5 and the difference of phase lags V3-V5 of the M_2 wave between extension of V5 in result (I - 1) and that of V3 in (IX - 1) are 3.09 and 2.74°, respectively.

If accurate estimates of V3/V5 and V3 - V5 are obtained via the analyses of long duration observations, we might be able to determine the tendency of the tidal extension by observations of V3 only.

2.1. Cavity effect on the diameter of cross-section of the tunnel.

Extension of the diameter of a circular hole in a plate with uniform tensile force in a azimut.

Since the Earth tide observatory is located close to the Earth's surface, we may consider only the horizontal component of the tidal stress when calculating the plane strain on the cavity effect by the tunnel. Let x and y be the horizontal and vertical axes, respectively, where the origin of the coordinates is at the centre of the cross-section. Let u and v be their displacement components due to the stress. Applying a uniform tensile force, p, in the x-direction on a thin plate of which Poisson's ratio is ν, u and v are :

$$2\mu u = (p/2)\, r' \left[\{(.1 - \nu) / (1 + \nu) + (a'/r')^2\} + \{1 + 4\,(a'/r')^2 / (1 + \nu) - (a'/r')^4\} \cos 2\alpha\right],$$

$$2\mu v = -\,(p/2)\, r' \{1 + 2\,(1 - \nu)\,(a'/r')^2 / (1 + \nu) + (a'/r')^4\} \sin 2\alpha \qquad (2)$$

where μ, a', r' and α are the rigidity, the radius of the hole, the distance from the centre of the hole and the deflection from the x-axis, respectively.

From equation (2), when $\nu = 1/4$, we have relative extensions, u/r' on the horizontal and the vertical radii on the hole (r' = a') as $4.8p/\mu$ and - 1.6 p/μ, respectively. And we also have their extensions, u/r' at $r' = \infty$ as 1.60 p/μ and - 0.40 p/μ, respectively. Namely, extension of the diameter, u/r' at x = a' and y = 0 is 3 times u/r' at $x = \infty$ and y = 0. And contraction u/r' at x = 0 and y = a' is 4 times u/r' at x = 0 and $y = \infty$. So, we can observe the large contraction on the vertical diameter of the cross-section of the tunnel instead of the small contraction at infinity.

3. Topographical effect

The topographical effect at Osakayama observatory is calculated by M. Hashida (1980) by means of J. Berger et al. formulas (1976) as follows,

$$e_s(\theta\,\theta) = 1.113e_h(\theta\,\theta) + 0.066e_h(\phi\phi) - 0.144e_h(\theta\phi)$$

$$e_s(\phi\,\phi) = -\,0.096e_h(\theta\,\theta) + 0.756e_h(\phi\phi) - 0.104e_h(\theta\phi)$$

$$e_s(\theta\,\phi) = -\,0.133e_h(\theta\,\theta) - 0.129e_h(\phi\phi) + 0.845e_h(\theta\phi) \qquad (3)$$

where e_h is the homogeneous strain which consists of the direct tidal effect and the oceanic load tide and e_s is the site strain which is affected by topography. Indices $\theta\theta$, $\phi\phi$, $\theta\phi$ of e_h or e_s correspond to the N-S and E-W normal strains and shear strain in the horizontal plane, respectively.

The M_2 wave of the site strain component at Osakayama has been observed by I. Ozawa (1996) as follows :

$$e_s(\theta\theta) = (0.5757 \cos 2t + 0.2993 \sin 2t) \times 10^{-8}$$

$$e_s(\phi\phi) = (0.6810 \cos 2t + 0.0677 \sin 2t) \times 10^{-8}$$

$$e_s(\theta\phi) = (-0.5427 \cos 2t - 0.2598 \sin 2t) \times 10^{-8} \qquad (X)$$

From (3) and (X) the components of the homogeneous strain is calculated as follows,

$$e_h(\theta\theta) = (0.3976 \cos 2t + 0.2252 \sin 2t) \times 10^{-8}$$

$$e_h(\phi\phi) = (0.8708 \cos 2t + 0.0813 \sin 2t) \times 10^{-8}$$

$$e_h(\theta\phi) = (-0.4314 \cos 2t - 0.2522 \sin 2t) \times 10^{-8} \qquad \text{(XI)}$$

From (X) the horizontal areal component of the site strain, $e_s\,\theta\theta + e_s\,\phi\phi$ is :

$$e_s(\theta\theta) + e_s(\phi\phi) = 1.3092 \times 10^{-8} \cos(2t - 16.28°) \qquad \text{(XII)}$$

From (XII) the areal component of the homogeneous strain, $e_h\,\theta\theta + e_h\,\phi\phi$ is :

$$e_h(\theta\theta) + e_h(\phi\phi) = 1.3049 \times 10^{-8} \cos(2t - 13.58°) \qquad \text{(XIII)}$$

It appears that the areal component of the homogeneous strain (XIII) is nearly equal to that of the site strain component (XII). Thus, the topographical effect on the areal component of the tidal strain cancelles out. The vertical component of the tidal strain is related to the areal component as follows,

$$e_{rr} = \sigma / (\sigma - 1).\ \{e_{\theta\theta} + e_{\phi\phi}\} \qquad (4)$$

where σ is the Poisson's ratio. From (4) we can evaluate e_{rr} :

$$e_{rr} = 0.4152 \times 10^{-8} \cos(2t - 193.58°) \qquad \text{(XIV)}$$

We determine that this value is not affected by topography. Since this value is nearly equal to the observed value, (I - 1).

Summary

1. The tidal vertical extensions in the well have been observed in the old Osakayama tunnel and the 8 main waves of the tidal strain are analysed from 55,026 hourly values. Then the oceanic load tide is subtracted from the observed value. Furthermore, the radial gradient of the Love's number, $a\partial h_2 / \partial r$ is evaluated for the M_2 wave.

2. Considering the loading due to the atmospheric tide, the effect of the solar heat radiation on the S_2 wave is evaluated from (I - 4).

3. The observations of the vertical extensions on the vertical diameter of the cross-section of the Osakayama tunnel have been analysed. The 8 main waves of the tidal strain are obtained.

4. The tidal extension of the diameter of the cross-section is amplified about 4 times by the cavity effect. According to the comparison between observations in the borehole and on the vertical diameter, the contraction along the vertical diameter is amplified 3.09 times.

5. Comparing the observed value of the tidal strain components and the site strain components which are modified, the topographical effect, we confirm that the topographical effects are cancelled on the horizontal areal strain and the vertical extension.

Acknowledgements

The author wishes to express many thanks to Professor Melchior for his valuable advices and helps of computations of the results, and to Dr. Van Dam for her corrections of English sentences.

References

Berger, J. & Beaumont, C, 1976.
An analysis of tidal strain observations from the United States of America, II. The homogeneous tide, Bull. Seismological Society, America, Vol. 66, 1821-1840.

Farrell, W.E., 1972.
Deformation of the Earth by surface loads, Reviews of Geophysics and Space Physics, Vol. 10, 761-797.

Hashida, M., 1980.
Considerations of Earth tidal strain in the Osakayama tunnel and observation of long extensometer, Thesis of Master course of Kyoto University.

Nishida, H., 1980.
Improved Tidal Charts for the Western Part of the North Pacific Ocean, Report of Hydrographic Researches n° 65, 55-70.

Ogura, S., 1933.
The Tides in the Seas adjacent to Japan, Bulletin Hydrographic Department, 7, 1-189.

Ozawa, I., 1974.
Types and distribution patterns of Earth tides, Journal of the Geodetic Society of Japan, Vol. 20, 178-187 (in Japanese).

Ozawa, I., 1984.
The Observations of the Earth Tidal Strains in Old Osakayama Tunnel, Bulletin Disaster Prevention Research Institute, Kyoto University, Vol. 34 Parts 4, n° 308, 169-186.

Ozawa, I., 1986.
On the observations and the interpretations of S_2 component on the Earth tides, Journal of the Geodetic Society of Japan, Vol. 32, 1-11.

Ozawa, I., 1996.
Ratio of tidal constants, Love's numbers h/l, Abstracts, Japan Earth and Planetary Science joint meeting, 605.

Schwiderski, E.W., 1980.
On Charting Global Ocean Tides, Review of Geophysics and Space Physics, Vol. 18, 234-268.

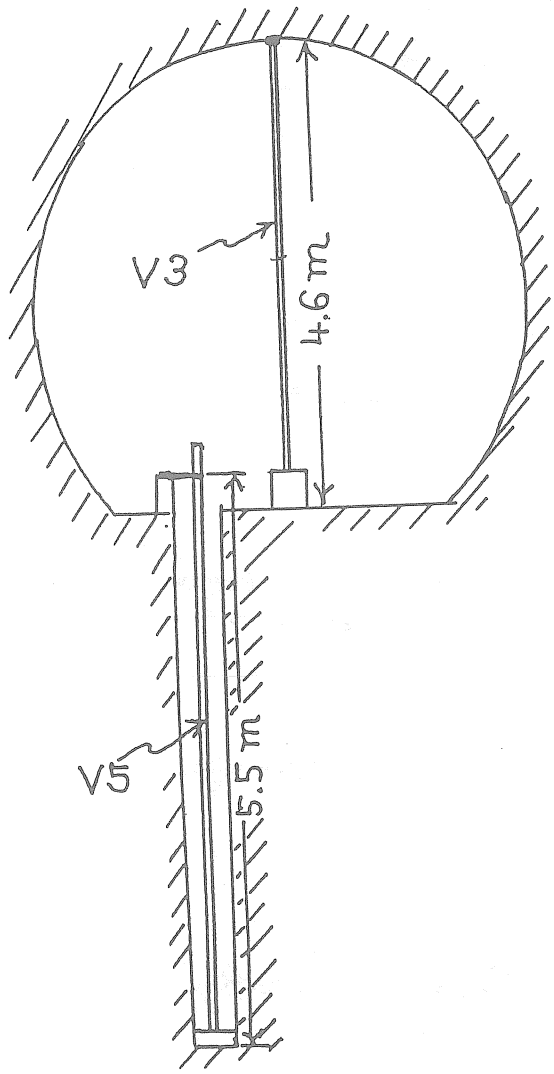

Fig.1. Schema of settings of vertical component of the extensometers, V3 and V5 in the old Osakayama tunnel.

V3 : invar rod, diameter 10 millimeters

V5 : super-invar pipe, outer diameter 35 millimeters inner diameter 30 millimeters.

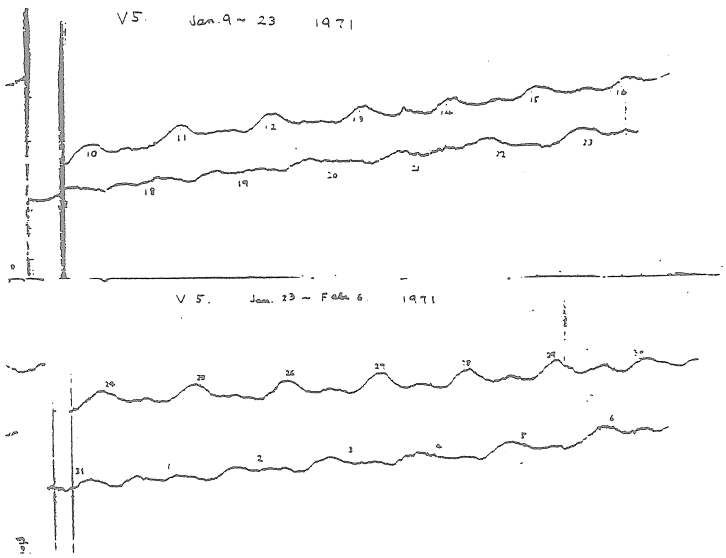

Photo. 1.(a). Photographic records of vertical component of extensometer, V5 in borehole in old Osakayama tunnel. A earthquake is seen in Jan. 10 in 1971.

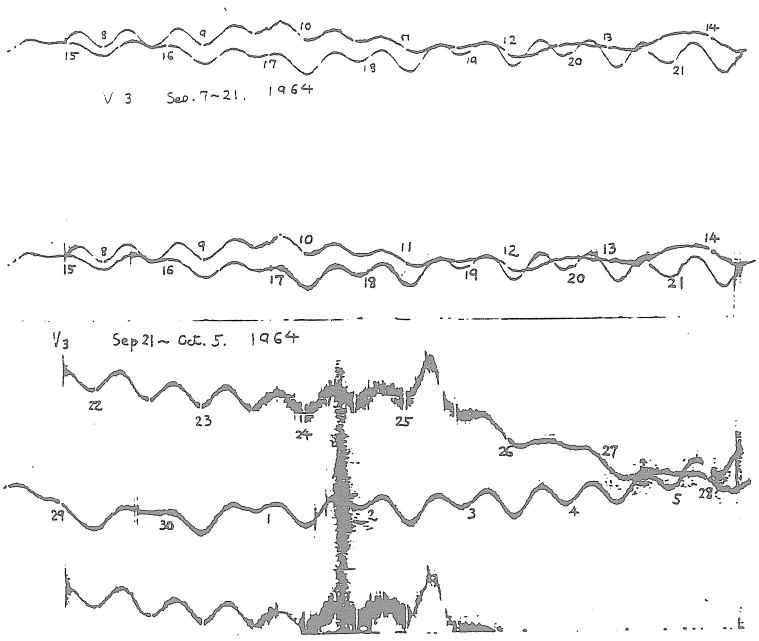

Photo. 1.(b). Photografic records of vertical component of extensometer, V3 on the vertical diameter of cross-section of the Osakayama tunnel. Effects of low atmospheric pressure and rain are seen in the period of Sep. 23~27. Earthquakes are seen in Sep. 22, Sep. 29, Oct. 1 and Oct. 5 in 1964.

VERTICAL TIDAL STRAINS IN UNDERGROUND CAVITIES

P. Melchior
Observatoire Royal de Belgique

The recent translation of papers, unknown to us, up to now, by Balavadze et al. (BIM 129) and by Uruchadse, (both from the Bulletins of the Academy of Sciences of Georgia) (the present BIM) and the publication of a paper by I. Ozawa in the present BIM, both related to vertical extensometers raised some new interest for these instrument whose results are rarely reported in the literature.

To our knowledge data from only three stations are presently available concerning vertical tidal strains.

0254 - Walferdange Grand Duchy of Luxembourg - 10 km north of Luxembourg City

$\varphi = 49.6647°$ N, $\lambda = 6.1500°$ E, depth 90 m, D = 270 km.

- old gypsum mine, gallery pierced into rather poorly consolidated gypsum, containing marls (Keuper strata), length 800 m; width to height ratio : r = 2
- quartz tube extensometer, 3.40 m length, outer diameter 60 mm, inner diameter 54 mm;
- 20 years measurements, 1971 - 1992, 113 424 hourly values.

1190 - Tbilissi, Georgia

$\varphi = 41.7167°$ N, $\lambda = 44.7833°$ E, depth 60 m, D = 3000 km.

- gallery pierced into granular sandstone, thin schist, tuff and clay;
- quartz tube extensometer, 6.50 m length;
- 506 days of measurements (1984 - 1986).

2820 - Osakayama Japan - 10 km from Kyoto City

$\varphi = 34.9833°$ N, $\lambda = 135.850°$ E, depth 150 m, D = 65 km.

- old railway tunnel, 700 m length, clay slate and shale belonging to the Chichibu Palaeozoic era;
- super invar pipe extensometer V5, 5.50 m length, outer diameter 35 mm, inner diameter 30 mm;
- 22 years measurements 55 026 hourly values;
- invar rod extensometer V3, 4.60 m length, diameter 10 mm;
- 30 years observations.

D is the distance to the nearest mesh of the M_2 oceanic cotidal map.

The lengths of the vertical extensometers usually correspond to the available vertical space of the galleries. Thus the ratios of the terrain coverages above the galleries (depth) to the galleries vertical dimensions are respectively 26 and 32 at Walferdange and at Osakayama but only 9 at Tbilissi.
A high ratio ensures that the cavity is sufficiently far from the boundary to avoid a distortion of the strain field (Harrison, 1976).

Theory

Vertical strain is proportional to $D/ag = 4.200\ 10^{-8}$ where D is the Doodson constant, a the Earth mean radius and g the mean gravity.
Semi-diurnal waves are proportional to $\cos^2 \varphi$ while the M_2 coefficient is 0.90812 in the tidal potential development. This gives a M_2 radial amplitude of $1.598\ 10^{-8}$ at Walferdange, $2.124\ 10^{-8}$ at Tbilissi and $2.560\ 10^{-8}$ at Osakayama.
The observed amplitudes in these stations are respectively $0.748\ 10^{-8}$, $0.645\ 10^{-8}$ and $0.588\ 10^{-8}$ (1966), $0.464\ 10^{-8}$ (1998) from which results an amplitude ratio

$\eta = -0.468$ at Walferdange
$\eta = -0.304$ at Tbilissi
$\eta = -0.230$ at Osakayama (1966)
$\eta = -0.181$ at Osakayama (1968).

η is called the vertical strain factor. It is defined as follows, in function of h, , the Love and Shida numbers, the h derivative with respect to the Earth's radius and the Poisson coefficient σ (Melchior 1983) :

$$\eta = a\, dh/dr + 2h = 2\sigma/(1 - \sigma)\ (3\ell - h)$$

from which we obtain

$$\sigma = \eta/(\eta + 6\ell - 2h)$$

$$ah' = \eta - 2h \qquad h' = dh/dr$$

The Poisson coefficient is also defined as

$$\sigma = \lambda/(\lambda + 2\mu) = 1 - 2\ (\beta/\alpha)^2$$

where λ, μ are the Lamé coefficients, α and β the speeds of P and S seismic waves.

Of course to obtain the numerical value of η as the ratio between the observed amplitude and the amplitude on a model Earth, we cannot use a rigid Earth model as we do for tidal tilts or tidal gravity changes.

To reduce the Walferdange data we, at the Royal Observatory, have taken as reference model an incompressible earth (thus $\sigma = 0.5$) with conventional Love numbers

$$h = 0.599 \qquad \ell = 0.083 \qquad 6\ell - 2h = -0.700$$

These are the Love numbers given by Dehant et al. (1998) for an inelastic non hydrostatic model earth.

Anyway, other h, ℓ acceptable values give $6\ell - 2h \approx -0.7$. In the Table I we compare different conventional models.

Table I **Reference Models**

incompressibility	$\sigma = 0.50$	$\eta = 6\ell - 2h = -0.700$	$ah' = -1.898$
$\lambda = 2\mu$	$\sigma = 0.33$	$\eta = 3\ell - h = -0.350$	$ah' = -1.548$
$\alpha = 6.10$ km s^{-1} $\beta = 3.54$ km s^{-1}	$\sigma = 0.326$	$\eta = 0.967\ (3\ell - h) = -0.338$	$ah' = -1.536$
$\lambda = \mu$	$\sigma = 0.25$	$\eta = 2/3\ (3\ell - h) = -0.233$	$ah' = -1.431$
Takeuchi	$\sigma = 0.25$	$\eta = -0.237$	$ah' = -1.477$
Molodenski I	$\sigma = 0.33$	$\eta = -0.343$	$ah' = -1.563$
Melchior at al.	$\sigma = 0.25$	$\eta = -0.232$	$ah' = -1.472$

Table II - Most recent results reported for the M_2 wave

	η	$\sigma = \eta/(\eta - 0.70)$	ah'	h' (10^{-4} km^{-1})
Walferdange	-0.465 ± 0.002	0.399	- 1.663	- 2.61
Tbilissi	-0.300 ± 0.026	0.294	- 1.498	- 2.35
Osakayama				
1966	-0.230 ± 0.036	0.247	- 1.428	- 2.24
1998	$-0.181 \pm$	0.205	- 1.379	-2.16

The M_2 phase at Walferdange is $+ 2.54° \pm 0.23°$ (lead)
and at Osakayama $- 5.36° \pm ?$ (lag)
it has not been published for Tbilissi.

Discussion

- Considering the difficulty of installation and maintenance of such instruments one may be satisfied to obtain amplitudes with rather small mean square errors and phases not too different from zero.

Moreover it is quite interesting to note that the M_2 phase at Walferdange (2.54°) coincides almost perfectly with the M_2 phase obtained in the same component but with the gravimeters (2.17° ± 0.01°).
Itsueli et al. (1975) also observed a close agreement between the observed and predicted phases at Queensbury station (no more than 10° difference).

- Cavity effects obviously contribute to the tidal strains. However computations conducted for galleries of similar size by Kovtunenko and Lyubushin (1996), Kovtunenko et al. (1998) and by Kostecky and Kohut (1998) as well show that, if the vertical amplitudes are increased, the phase is practically not affected : see figures 7a, b in the first of these papers, figure 3 in the second paper and the different figures in the third paper. The main disturbances due to cavity effect occur in the corners of trapezoidal cavities and lateral walls (Harrison, 1976; see also Table 1 in Kostecky and Kohut paper) where vertical extensometers are not normally installed while the roof and floor remain flat despite stress concentration.

- One may consider that for compacted rocks at the earth's surface, the Poisson coefficient could have a value close to 0.25 (Melchior et al. 1974) but that a higher value should not be inconsistent with the local structures : mining galleries with adjacent holes or rooms like at Walferdange and Tbilissi. Thus the values given in the Table II even if quite high do not seem to be really abnormal.
Of course, the radial derivative of the Love number h depends on the elastic properties of the upper crust and the surrounding rocks. Nevertheless there is some concordance for the numerical value of h' in the three stations.

- At Walferdange the diurnal waves show the resonance effect due to the liquid core as the ratios of η to η (O_1) correspond to the ratios of h to h (O_1) in the Dehant et al. (1998) models.

Table III

	η	phase	Ratios η to η (O_1)	Ratios h to h (O_1)
Q_1	0.457 ± 0.025	2.41° ± 3.09°	1.011	1.001
O_1	0.452 ± 0.005	1.20° ± 0.58°	1	1
P_1	0.401 ± 0.010	9.09° ± 1.43°	0.887	0.963
K_1	0.391 ± 0.003	4.21° ± 0.48°	0.865	0.864

(a positive phase corresponds to a lead)

- The stress caused by the atmospheric pressure variations (τ_{zz} = - P) directly acts on the vertical extensometer. It considerably amplifies the S_1 signal at the three stations and disturbs the tidal S_2 component as shown by the abnormal phases of this component at Walferdange (20°) and Osakayama (26°).

At Walferdange the S_1 phase is - 175.6° ± 8.5° while the phases of the O_1 diurnal wave is 1.2° ± 0.6° (Table III); the S_2 phase exhibits a large amplitude and a strong phase lag with respect to the M_2 wave :

M_2	$A = (7.48 \pm 0.03)\ 10^{-9}$	$\alpha = 2.13° \pm 0.23°$
S_2	$A = (4.16 \pm 0.03)\ 10^{-9}$	$\alpha = 19.89° \pm 0.42°$

If we proceed in the same way as Ozawa (1998 § 1.1), that is subtracting $0.46\ A\ (M_2) = 3.48\ 10^{-9}$ from $A\ (S_2)$, the S_2 anomaly results as

$$A = (1.49 \pm 0.04)\ 10^{-9} \qquad \alpha = 71° \pm 0.48°$$

The S_2 wave in the barometric pressure is very stable and amounts to 0.336 mbar with a phase - 131° at Findel Airport of Luxembourg (Delcourt 1986) which is practically 180° from the extensometer's phase while the amplitude ratio, i.e. the admittance of the extensometer to the barometric pressure is

$$(4.43 \pm 0.25)\ 10^{-9}\ /\text{mb}.$$

Urachadse (1989, translation in this Bulletin) found for the Tbilissi vertical strainmeter an admittance of

$$(4.98 \pm 0.67)\ 10^{-9}\ /\text{mb}$$

by analysis of the drift perturbations of this instrument.

A precise (if possible) calculation of the cavity effect on the vertical strains at these three stations would be helpful to check the properties of the rocks and the response of the instruments to different kinds of perturbations.

References

Balavadze, V.K., Kartvelichvili, K.Z. and Uruchadze, R.M., 1988.
Premiers résultats des observations avec l'extensomètre vertical en quartz à Tbilissi.
Bull. Acad. Sciences of Georgia, 129, 3, pp 541-544 (in russian).
Translation : Bull. Infor. Marées Terrestres 129, pp 9985-9988, 1998.

Dehant, V., Defraigne, P. and Whar, J-M., 1997.
Tides for a convective Earth.
13th Symposium on Earth Tides, Bruxelles : 261-263
J. Geoph. Res., submitted.

Delcourt-Honorez, M., 1986.
Lunar and solar barometric tides in seven stations of the Trans World Tidal Gravity Profiles.
Bull. Inf. Marées Terrestres, 97 : 6614-6627.

Harrison, J-C., 1976.
Cavity and Topographic Effect in Tilt and Strain Measurements.
J. Geoph. Res. 81 : 319-328.

Itsueli, U.J., Bilham, R.G., Goulty, N.R. and King, G.C.P., 1975.
Tidal Strain Enhancement Observed Across a Tunnel.
Geoph. J.R. Astron. Soc. 42 : 555-564.

Kostecky, P. and Kohut, I., 1998.
The estimation of the cavity effect by higher degree finite element approximation.
Studia Geophysica and Geodetica, 42, 1 : 61-80.

Kovtunenko, L.P. and Lyubushin, A.A., 1996.
Interpretation of Tidal and Barometric Deformations of a Tunnel.
Izvestiya, Physics of the Solid Earth, 32, 7 : 600-608.

Kovtunenko, L.P., Manukin, A.B. and Lyubushin, A.A., 1998.
Modelling of Tidal Deformations of a Gallery in a Poroelatic Medium.
Izvestiya, Physics of the Solid Earth, 34, 7 : 555-563.

Melchior, P., Ducarme, B., Van Gils, J-M., Flick, J. and Denis, C., 1974.
Preliminary results obtained with a vertical strainmeter at the Underground Laboratory of Geodynamics at Walferdange (Grand Duchy of Luxembourg).
Phys. Earth and Planetary Int., 9 : 97-100.

Melchior, P., 1983.
The Tides of the Planet Earth, 2nd edition.
Pergamon Press, 641 pages.

Ozawa, I., 1966.
On the Observations of the Tidal Strains at Osakayama Observatory.
Special Contrib. Geoph. Inst. Kyoto University 6 : 233-246.

Ozawa, I., 1998.
Observations of the Earth Tide Vertical Extension in the old Ozakayama tunnel.
Bull. Inf. Marées Terrestres 130.

Uruchadse, R.M., 1989.
Perturbations irrégulières de la dérive d'un extensomètre vertical en relation avec les variations de la pression atmosphérique.
Bull. Acad. Science of Georgia, 135, 2, pp 93-96 (in russian).
Translation : Bull. Infor. Marées Terrestres 130, pp , 1998.

Traduction

ETUDE DES DEFORMATIONS DE MAREES DE L'ECORCE TERRESTRE SELON LES OBSERVATIONS DEFORMOGRAPHIQUES A LA STATION DE KHOUDONI

B.K. Balavadze (Académicien),
V.G. Abachidse, R.M. Karmaleyeva,
L.A. Latinina, T.A. Tsagouria.

Communications de l'Académie des Sciences de Géorgie.
Vol. 125, n° 1, pp 61-64, 1987.

En 1980 l'Institut de Géophysique de l'Académie des Sciences de Géorgie a organisé sur la rive Est du réservoir d'eau d'Ingouri (anciennement S. Khoudoni une station géophysique équipée de clinomètres et de déformographes. Ces appareils sont situés dans une galerie d'une longueur de 60m avec une voie latérale. La galerie a été creusée perpendiculairement au flanc de la montagne constituée de porphyre et de tuff sablonneux.

Nous analysons dans cet article les résultats des observations de 1982 avec des déformographes à quartz équipés de transformateurs optico-mécaniques.

La figure 1 illustre le graphique des déformations enregistrées par les deux extensomètres réciproquement perpendiculaires, l'allure de la variation de la température de l'air d'après les données de la station météorologique locale Potskho-Etseri et le niveau de l'eau dans le réservoir.

Comme nous le constatons, pour la composante N19°E (~ N-S) on observe une dilatation et pour la composante E 9°10 (~ E-W) une compression des roches constituant le massif. Les vitesses des déformations de dilatation et de compression ne sont pas élevées et à peu près égales à $1,2.10^{-6}$/an. Ce qui est jusqu'à trois fois moindre que la vitesse des déformations obtenues d'après les données de la première station extensométrique fonctionnant sur la rive droite du fleuve Ingouri près du barrage ($3,0.10^{-6}$/an) [1, 2]. Ceci peut selon toute vraisemblance être expliqué d'une part par la structure tectonique du site - dans la région du barrage deux extensomètres installés parallèlement coupent la zone de fracture de même que dans la station de Khoudoni les appareils se trouvent sur le massif du côté de la fracture d'Ingiritch -, d'autre part, par l'influence du relief local - la galerie de la première station est construite au niveau de la base de la montagne et la seconde (station Khoudoni) est plus proche du sommet de la montagne.

Conformément aux calculs de Harrison [3] la déformation dans le massif diminue du pied de la montagne vers le sommet jusqu'à s'annuler ce qui explique la différence notée plus haut dans les valeurs des déformations observées dans la première et la seconde station. En même temps nous remarquerons que dans la seconde station les inclinaisons de la surface terrestre ne sont pas importantes - le total de l'année ne dépasse pas 2 à 2,5 sec. d'angle.

La comparaison des courbes de déformations et des variations du niveau de l'eau montre que la montée de l'eau dans le réservoir correspond à une croissance de la vitesse des déformations de dilatation suivant la direction NS et de compression pour la direction EW. Cela s'explique par la position locale de la station par rapport au réservoir: l'augmentation de la charge lors du remplissage du réservoir se produit dans le Sud du point d'observation

ce qui se remarque aussi par la dilatation des roches dans la direction NS. Dans le demi-espace homogène la déformation dans la direction transversale à l'effet de charge (EW) doit être voisine de zéro. La déformation observée dans cette direction résulte de la structure hétérogène de la région et de ses particularités géologiques.

L'influence de la déformation thermique est plus grande sur la composante NS que sur la composante EW puisque la crête montagneuse a une étendue voisine de la largeur et l'échauffement de sa pente Sud provoque une dilatation des roches dans la direction N.S. La déformation thermique par rapport à l'évolution de la température retarde en phase de deux mois. Le coefficient de corrélation entre la variation de la température de l'air et les déformations des roches est égal à 0.64 pour la composante NS et à 0.11 pour la composante EW.

On a fait l'analyse des ondes de marée luni-solaire selon la méthode de B.P. Pertsev [4]. Les calculs ont été faits avec un déplacement d'un jour. Les valeurs théoriques des amplitudes et des phases des ondes individuelles sont calculées pour une direction arbitraire par la formule:

$$l_{aa} = l_{\theta\theta}\, m^2 + l_{\theta\phi}\, mn + l_{\phi\phi}\, n^2$$

où $l_{\theta\theta}$ et $l_{\phi\phi}$ sont les composantes de la déformation dans les directions du méridien et du premier vertical, m et n sont les cosinus directeurs. La déformation est calculée avec les constantes élastiques pour les modèles de Terre actuels: h = 0,6 et ℓ = 0,07.

Comme le montre la table les amplitudes des ondes principales M_2 et O_1 atteignent en tout 20 à 35% de leurs valeurs théoriques. Les amplitudes de toutes les ondes individuelles étaient minimisées, S_2 et K_1 étant plus fortement perturbées par les effets théoriques ce qui témoigne de la nature non météorologique de la perturbation observée. Pour les ondes les plus sûres M_2 et O_1 les déphasages dans la direction NS sont importants et diffèrent sensiblement des valeurs théoriques. Cette direction est presque perpendiculaire à la pente de la crête et l'influence du relief est ici particulièrement grande. Dans la direction EW les déphasages sont moindres mais diffèrent cependant suffisamment fort des valeurs théoriques.

Les valeurs anormalement basses obtenues pour les amplitudes des ondes de marées d'après les données de la composante NS peuvent s'expliquer par la position de la station dans la partie supérieure de la pente de la crête montagneuse où conformément à Harrison, les déformation élastiques doivent diminuer d'à peu près trois fois en comparaison avec les valeurs non perturbées. La diminution des amplitudes des ondes de marées selon les composantes EW peut être provoquée également par l'influence de la zone de fracture d'Ingirich qui s'étend dans une direction à peu près perpendiculaire à l'axe de l'appareil. La station est située sur le bord de la fracture.

En conclusion nous noterons que les faibles valeurs des amplitudes observées pour les ondes de marées s'expliquent non seulement par l'influence du relief mais aussi par le fait que dans le massif où se font les observations il n'y a pas de déformations actives.

Les vitesses des déformations lentes sur la fracture et sur le monolithe latéral sont respectivement égales à $3{,}0.10^{-6}$ et $1{,}2.10^{-6}$ par an. Cette différence diminue un peu si on tient compte que l'influence du relief sur ces deux stations est proportionnelle à 2/3. Ainsi, le massif de la station de Khoudoni se déforme deux fois plus faiblement que dans la station d'Ingouri

Références.

1. Б. К. Балавадзе, А. Е. Островский, В. Г. Абашидзе, Л. А. Латынина. и др. Сб. «Современные движения земной коры». Новосибирск, 1976.
2. Б. К. Балавадзе, В. Г. Абашидзе, Н. А. Жариков, Л. А. Латынина, Э. Г. Шенгелая. Сообщения АН ГССР, 98, № 3, 1980.
3. J. C. Harrison. J. Geophys. Res; v. 81, № 2, 1976.
4. Б. П. Перцев. Изв. АН СССР, сер. геофиз., № 8, 1958.

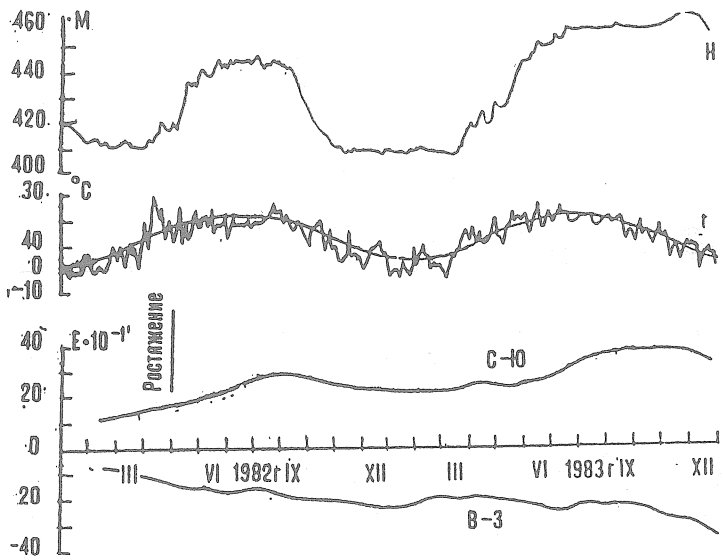

Figure 1 Graphique des déformations de l'écorce terrestre à la station de Khoudoni, de la variation de la température de l'air et du niveau de l'eau dans les réservoirs.

Amplitudes des ondes de marées

Jours moyens de la série	Déformographe	Amplitude en un . 10^{-9}					Phases $\Delta\phi°$				
		M_2	S_2	N_2	K_1	O_1	M_2	S_2	N_2	K_1	O_1
7.X.1982 r	N19°E	2,35	1,80	0,76	1,56	1,30	1,5	—46,3	12.9	—166.2	—158,3
13.X.1982 r	"	2,55	1,76	0,72	1,83	1,29	4,8	—47,9	31,1	—172.9	—143,0
8.XII.1982 r.	"	2,03	1,24	0,84	1,60	1,92	54,0	--56,2	30,0	—141,4	— 49,6
13.XII.1982 r.	"	2,05	1.47	0,96	1,79	1,81	54,4	—70,0	24,0	—129,4	— 55,5
moyenne	"	2,25	1,57	0,82	1,70	1,58	28,7	—59,1	24,5	—152,5	—101.7
valeur théo-	"	±0,21	±0,21	±0,08	±0,00	±0,29	±25,5	± 8,5	± 3,5	± 17,1	± 49,0
rique		11,47	5,33	2,20	6,82	4,84	13,5	13,5	13,5	14,7	14.7
7.X.1982 r.	E9°10	0.59	0,92	0,47	0,07	1,79	3,0	80.0	—47.6	--115,5	13.6
13.X.1982 r.	"	0.62	1,00	0,43	0,18	1,44	—10,0	74,0	125.6	—222,4	12,9
moyenne	"	0,61	0.96	0,45	0,12	1,62	— 3.9	77.0	39.0	—169.0	13.3
valeur théo-	"	±0.02	±0.06	±0.03	±0,08	±0.28	± 9.8	± 4.2	±122.0	± 75.5	± 0.5
rique		3,32	1.54	0,64	9.83	6.98	20,2	20.2	20.2	— 4.3	— 4.3

Traduction

DEFORMATIONS DE LA SURFACE DE LA TERRE ET VARIATIONS DU CHAMP GRAVITATIONNEL DUES A LA MONTEE DU NIVEAU DE LA MER CASPIENNE

B.P. Pertsev.

Institut de géophysique planétaire Schmidt, Moscou
Fizika Zemli 1996, n°3, pp 82-85.

Commençant en 1977, le niveau de la mer Caspienne, comme on sait [1], s'élevait continuellement et, à ce jour, dépassait sa valeur précédente d'à peu près 2m. Cela a dû sans aucun doute conduire à une déformation de la surface de la Terre et à une variation du champ gravitationnel dans les zones les plus proches de la mer Caspienne. Ce phénomène offre une possibilité exceptionnelle de comparer les résultats des calculs des déformations de la surface et des variations du champ de gravitation pour un modèle de Terre aux mesures gravimétriques répétitives et de préciser à l'échelle de la région la structure des couches supérieures de la Terre et le caractère des mouvements actuels de l'écorce terrestre. En outre, étant donnée la durée de ce phénomène unique, les mesures géodésiques répétitives permettent de donner une estimation du creep du manteau supérieur. Nous nous sommes limités dans ce travail à l'estimation des valeurs des fléchissements possibles de la surface de la Terre, des déformations des surfaces de niveau et des valeurs de la force de pesanteur, ne faisant aucune hypothèse sur les causes de l'apparition de la couche d'eau additionnelle de deux mètres. Dans le cas considéré nous nous sommes basés sur des causes climatologiques et non géologiques de l'apparition de ce phénomène [1].

Comme il a été montré en [2], la solution du problème classique de Boussinesq a donné des résultats nettement exagérés lors de la détermination des fléchissements de la surface du modèle de Terre. De plus le problème de Boussinesq est un problème de la théorie de l'élasticité où on ne tient pas compte de la variation du champ de gravitation de la Terre. C'est pourquoi, dans notre estimation, nous nous sommes tournés vers la méthode appliquée pour le calcul de l'influence de l'effet indirect des marées océaniques sur les marées terrestres où, outre les propriétés élastiques, on tient compte de la force de gravitation et également de la sphéricité et de l'hétérogénéité de la Terre [3].

Pour un modèle de Terre à symétrie sphérique, élastique, hétérogène, compressible et en gravitation, comme nous le savons [4], tous les phénomènes de marées se produisant à la surface de la Terre et dans le corps de la Terre, peuvent être décrits à l'aide des nombres élastiques de Love et Shida h_n, k_n et l_n et des coefficients de charge $\overline{h}_n$, $\overline{k}_n$ et $\overline{l}_n$. Ces derniers décrivent la déformation de la sphère terrestre sous l'effet de charge de surfaces gravitantes, représentées par une couche simple dont le potentiel est donné en série de fonctions sphériques. La valeur de ces paramètres est déterminée par la solution du système d'équations différentielles du 6ème ordre, décrivant l'équilibre de la sphère élastique gravitante, déformée par une force dont le

potentiel à l'intérieur de la sphère est un polynôme harmonique homogène. En particulier la force génératrice de marées possède cette propriété. Les nombres de Love et Shida et également les coefficients de charge dépendent de la répartition de la densité et des propriétés élastiques à l'intérieur de la Terre.

Dans nos calculs nous sommes partis de la représentation de la Terre par le modèle actuel PREM [5] pour lequel nous avons calculé jusqu'à un ordre élevé n les nombres de charge de Love et Shida. Le calcul des coefficients de charge jusqu'à un ordre de quelques dizaines de milliers est nécessaire pour garantir la possibilité de construction des fonctions de l'influence des segments de petite surface et par cela même donne la possibilité de calculer l'effet des zones voisines et des petits détails de la géométrie du contour compliqué de la couche de charge d'eau de mer.

Dans le modèle de Terre PREM comme d'ailleurs aussi dans la plupart des autres, les valeurs de la densité, des paramètres élastiques et de la force de pesanteur sont données en fonction de la profondeur. Pour l'intégration numérique du système d'équations différentielles nous avons représenté les variations de ces paramètres avec la profondeur sous forme de fonctions continues, en conservant les sauts uniquement aux limites du noyau principal et du noyau interne. Dans ce but les répartitions données en [5] en fonction du rayon, de la densité, de la force de pesanteur et des paramètres élastiques μ et λ ont été approximées par 23 paraboles dans le manteau, onze dans le noyau externe et six dans le noyau interne. En fonction de la répartition de la densité donnée sous cette forme on a calculé, à titre de contrôle, la masse et le moment d'inertie du modèle de Terre. Pour simplifier l'intégration du système d'équation, la partie centrale du noyau interne jusque 3% du rayon terrestre a été considérée comme homogène et incompressible.

Comme on le sait [4], on a une solution analytique pour le noyau. L'intégration numérique du système d'équations a été faite par la méthode de Runge-Kuta avec un pas variable. Pour les ordres inférieurs de n l'intégration a été faite depuis le centre vers l'extérieur en commençant par un noyau homogène incompressible dont le rayon croissait à mesure de l'augmentation de l'ordre n. Le calcul de l'effet du noyau liquide pour des petites valeurs de n a été réalisé sans calcul séparé de la fonction auxiliaire introduite en [4].
En supposant que dans le noyau principal la valeur du module de rigidité μ est différente de zéro mais de quelques ordres plus petite que dans le manteau, on peut déterminer les paramètres cherchés par l'intégration du système d'équations depuis la limite du noyau interne incompressible jusqu'à la surface extérieure de la sphère terrestre. Les calculs effectués ont montré qu'en simplifiant de cette façon les calculs nous n'avons pas perdu en précision les nombres usuels ou de charge de Love et Shida. Mais à partir de n = 25 l'intégration a été faite depuis la surface extérieure de la sphère terrestre vers l'intérieur. Dans ce cas, avec l'augmentation de l'ordre n la profondeur de l'intégration a diminué. Pratiquement cela se ramène au fait qu'à mesure de la croissance de n, le rayon du noyau homogène incompressible a augmenté, s'approchant de la surface de la Terre. La profondeur jusqu'à laquelle on a fait l'intégration a été déterminée par calcul. Et pour ne pas perdre ainsi en précision on a diminué les dimensions des pas d'intégration et on a augmenté leur nombre. Etant donnée la variation adoucie des coefficients de charge aux ordres élevés de n, les calculs de ces paramètres n'ont naturellement pas été faits pour tous les ordres. L'intervalle a augmenté à mesure de la croissance de l'ordre n. La méthode de calcul des coefficients

de charge et des nombres usuels de Love et Shida est proposée en détail en [3]. Les valeurs obtenues par les calculs des nombres de Love et Shida pour n = 2, 3, 4 et des paramètres de charge pour les ordres choisis de n sont donnés dans les tables 1 et 2.

Sur la base des coefficients de charge calculés, les fonctions de Green (ou plutôt les fonctions d'influence des segments sphériques de surface de 0°1 x 0°1) nécessaires pour résoudre les problèmes posés ont été recalculées pour les différentes distances sphériques ψ.

On sait que les flexions de la surface de la Terre, pour un modèle terrestre élastique à symétrie sphérique provoquées par la charge d'une couche homogène d'eau de mer recouvrant un segment sphérique de rayon α, peut s'écrire sous la forme suivante [2]:

$$\Delta H = \frac{2\pi f \rho a}{g} \sum_{n=0}^{\infty} \frac{\bar{h}_n}{2n+1} [P_{n-1}(\alpha) - P_{n+1}(\alpha)] P_n(\psi),$$

où f est la constante d'attraction, ρ est la densité de l'eau de mer, a est le rayon de la Terre, g est la force d'attraction à sa surface, P_n sont les fonctions sphériques d'ordre n d'arguments α et ψ. Ici α est le rayon sphérique du segment et ψ est la distance depuis le centre du segment jusqu'au point d'observation. Après avoir remplacé dans cette expression h_n par $(1 + k_n - h_n)$ nous obtiendrons la formule pour le calcul de la fonction d'influence du segment décrivant le déplacement de la surface de niveau du champ gravitationnel par rapport à la surface de la Terre sous l'effet de la même charge.

Enfin, la fonction d'influence du segment décrivant la variation de la force de pesanteur s'écrit comme suit [6],

$$\Delta g = -8\pi f \rho G(\alpha, \psi) + \frac{\pi f \rho (1 - \cos\alpha)}{2\sin(\psi/2)} A(h, \psi),$$

où

$$G(\alpha, \psi) = \frac{1}{2} \sum_{n=0}^{\infty} \frac{\bar{h}_n - (n+1)\bar{k}_n/2}{2n+1} \times \times [P_{n-1}(\alpha) - P_{n+1}(\alpha)] P_n(\psi),$$

mais

$$A(h, \psi) = \frac{1 + h/2a\sin^2(\psi/2)}{\left(1 + \frac{h}{a} + h^2/4a^2\sin^2(\psi/2)\right)^{3/2}}.$$

Comme on le constate par ces formules, lors du calcul de la force de pesanteur, la composante de l'attraction ne dépendant pas de la structure de la Terre se calcule séparément des composantes dépendant de la déformation de la sphère terrestre sous l'effet de la charge gravitante. Cela permet de tenir compte, à l'aide de la fonction A (h, ψ), de l'influence de la hauteur h du point d'observation par rapport au niveau de la couche d'eau de mer sur les valeurs de la force de pesanteur. Comme on l'a montré en [6] la valeur A(h, ψ)

ψ) peut exercer une influence sensible sur les résultats pour les hauteurs h $\geq$ 200 m et de faibles distances sphériques ψ. Dans nos travaux n'ayant pour but que de donner l'estimation de l'effet nous n'avons pas précisé les valeurs des hauteurs des points de départ individuels et nous avons pris pour tous les points h = 100 m étant convaincus que les petites variations des hauteurs prises n'influencent pas nos résultats. De plus, dans les régions indiquées au Nord et à l'Est de la mer Caspienne la surface de la Terre ne diffère pas par de grandes altitudes.

Après s'être servi des fonctions calculées de l'influence des segments et après avoir partagé la surface de la mer Caspienne en 230 trapèzes de différentes grandeurs, bordant et englobant toute la mer, on a fait le compte des déplacements radiaux (dans le cas donné des fléchissements) de la surface de la Terre, des déplacements de la surface de niveau et des variations des valeurs de la force de pesanteur déterminées par l'effet de la charge d'une couche de deux mètres d'eau couvrant cette mer. Les calculs ont été faits pour les points de deux profils s'éloignant au Nord et à l'Est de la mer Caspienne de 300 km suivant le méridien de 50° et suivant le 44ème parallèle. Les résultats des calculs sont donnés dans les tables 3 et 4. Là également sont indiqués les flexions de la surface de la Terre calculés par la solution du problème de Boussinesq.

Dans ces calculs on a pris les valeurs en surface des modules d'élasticité μ et λ pour le modèle de Terre PREM (troisièmes colonnes des tables). Si on prend les modules d'élasticité pour le modèle de Terre n° 508 de Gilbert et Dziewonski [7] on obtiendra alors des résultats jusqu'à 2 fois plus grands. Ayant pris les modules d'élasticité depuis la couche de surface du modèle de Terre de Gutenberg [8], nous obtenons des fléchissements 20% plus petits. Enfin on a pu obtenir n'importe quelle autre solution, après avoir pris d'autres valeurs des paramètres élastiques et de même en introduisant un autre facteur constant dans la solution de Boussinesq. Dans les quatrièmes colonnes des tables 3 et 4 nous donnons les résultats obtenus pour μ et λ correspondant à la profondeur de 670 km du même modèle de Terre PREM.

Sont donnés en outre dans les tables de comparaison les fléchissements et les variations de la force de pesanteur obtenus en utilisant les paramètres de charge pour le modèle de Terre n° 508 de Gilbert et Dziewonski [7]. Les résultats diffèrent des résultats obtenus selon le modèle de PREM en tout de quelques pour cents.

Comme il résulte des tables, la montée considérée du niveau de la mer donne des valeurs tout à fait perceptibles aussi bien pour les fléchissements de la surface de la Terre que pour les variations de la force de pesanteur. En outre toutes les valeurs indiquées décroissent assez rapidement à mesure de l'éloignement du point d'observation du rivage de la mer. La diminution des fléchissements dans notre solution se produit sensiblement plus rapidement que dans le cas de la solution du problème de Boussinesq. C'est pourquoi il n'est pas possible de réunir des modules de μ et λ afin de faire coïncider suivant tout le profil la solution du problème de Boussinesq avec la solution obtenue à l'aide des fonctions d'influence des segments. Nous noterons également que, comme il résulte des tables 3 et 4, les déplacements de la surface de niveau et de la force de pesanteur sont presque deux fois plus grands que les fléchissements de la surface de la Terre sous l'effet de la même charge gravitante.

Enfin, lors des calculs nous n'avons pas tenu compte de ce que l'augmentation du niveau de la mer conduit à l'envahissement d'une partie du terrain. Ces domaines n'ont pas été pris en considération dans les calculs ce qui peut sans aucun doute perturber dans une certaine mesure les résultats finaux.

Notre travail a été réalisé avec le soutien du Fonds Scientifique International (subside NFE - 000).

Bibliographie

1. *Голубов Б.Н.* Аномальный подъем уровня Каспийского моря и техногенная дестабилизация недр // Изв. РАН. Сер. Географическая. 1994. № 1. С. 59–74.
2. *Перцев Б.П., Иванова М.В.* Вертикальные смещения земной поверхности под действием нагрузки морских приливов // Изучение земных приливов. М.: НАУКА. 1980. С. 48–53.
3. *Перцев Б.П.* Влияние морских приливов ближних зон на земноприливные наблюдения // Изв. АН СССР. Сер. Физика Земли. 1976. № 1. С. 13–22.
4. *Молоденский М.С.* Упругие приливы, свободная нутация и некоторые вопросы строения Земли // Труды Геофизического ин-та АН СССР. 1953. № 19(146). С. 3–52.
5. *Dziewonski A., Anderson D.* Preliminary reference Earth model // Phys. Earth Planet. Interiors. 1981. V. 25. № 4. P. 297–356.
6. *Перцев Б.П., Иванова М.В.* Оценка влияния нагонных вод на значения силы тяжести и высоты земной поверхности в прибрежных районах // Изв. АН СССР. Сер. Физика Земли. 1981. № 1. С. 87–91.
7. *Gilbert F., Dziewonski A.* An application of normal mode theory to the retrieval of structural parameters and source mechanisms from seismic spectra // Phil. Trans. Roy. Soc. London. Ser. A. V. 278. №. 1280. 1975. P. 187–269.
8. *Alterman Z., Jarosch H., Pekeris C.* Propagation of Rayleigh waves in the Earth. // Geophys. J. 1961. V. 4. P. 219–241.

Table 1. Nombres de Love et de Shida pour le modèle de Terre PREM.

n	h_n	k_n	l_n
2	0.60714	0.30015	0.08495
3	0.29024	0.09284	0.01517
4	0.17675	0.04188	0.01052

Table 2 Coefficients de charge pour le modèle de la Terre PREM.

n	$-\bar{h}_n \times 10^4$	$-n\bar{k}_n \times 10^4$	$n\bar{l}_n \times 10^4$	n	$-\bar{h}_n \times 10^4$	$-n\bar{k}_n \times 10^4$	$n\bar{l}_n \times 10^4$
0	1323.2	0	0	25	21831	11653	5442.8
1	2865.9	0	1026.9	30	23302	12553	6164.7
2	9951.9	6139.7	444.96	50	26704	14346	7936.3
3	10557	5921.9	2076.3	100	30131	15056	9160.6
4	10595	5394.8	2316.9	200	34846	15701	9120.1
5	10937	5292.2	2267.1	500	48029	21694	11438
6	11526	5487.3	2264.2	1000	59029	28444	16726
7	12226	5823.6	2335.0	3000	62304	30655	18914
8	12957	6215.4	2452.9	10000	62322	30681	18914
10	14382	7030.5	2754.6	50000	62328	30691	18913
15	17475	8910.7	3648.8	80000	62328	30689	18913
20	19926	10454	4587.3				

Table 3 Déplacements radiaux (ΔH), déplacements de la surface de niveau (ΔΓ) et variations de la force de pesanteur (ΔG) le long du méridien de longitude 50°

№№	Latitude	ΔH, см				ΔΓ, см	ΔG, μГл	
		Boussinesq		PREM	508	PREM	PREM	508
1	47.0	8.5	1.8	1.7	1.9	3.0	4.9	4.9
2	47.5	7.1	1.5	1.25	1.3	2.3	3.6	3.7
3	48.0	6.1	1.3	0.95	0.97	1.8	2.8	2.8
4	48.5	5.4	1.2	0.75	0.76	1.5	2.3	2.3
5	49.0	4.9	1.05	0.62	0.62	1.3	2.0	1.9
6	49.5	4.5	0.96	0.52	0.52	1.2	1.7	1.7

Table 4 Déplacements radiaux (ΔH), déplacements de la surface de niveau (Δr) et variations de la force de pesanteur (ΔG) le long du parallèle de latitude 44°.

№№	Longitude	ΔH, см				Δr, см	ΔG, μГл	
		Boussinesq		PREM	508	PREM	PREM	508
1	51°2	12.2	2.6	2.8	3.4	4.6	7.7	7.7
2	51.9	10.7	2.3	2.2	2.3	3.8	6.2	6.4
3	52.6	9.6	2.1	1.8	1.9	3.2	5.2	5.3
4	53.3	8.7	1.9	1.5	1.6	2.8	4.4	4.4
5	54.0	7.9	1.7	1.3	1.3	2.4	3.8	3.7
6	54.7	7.2	1.5	1.1	1.1	2.1	3.3	3.2

Traduction

ANALYSE HARMONIQUE DES INCLINAISONS DE MAREES DANS LA REGION D'INGOURI

V.G. Abachidse, Y.A. Melkadse

Présenté par l'Académicien B.K. Balavadse 10.5.1967
Bulletin de l'Académie des Sciences de Géorgie
130, n° 1, pp 77-80, 1988.

Les études des inclinaisons de marées de l'écorce terrestre provoquées par l'attraction luni-solaire donnent la possibilité de déterminer les constantes élastiques de la Terre γ et $\Delta\phi$.
Le facteur d'amplitude γ représente le rapport de l'amplitude observée des inclinaisons de marées de l'onde étudiée $A_{obs.}$ par rapport à l'amplitude calculée $A_{théor.}$ et caractérise la flexibilité de la partie supérieure de la Terre sous l'effet des forces génératrices de marées de la Lune et du Soleil. La valeur $\Delta\phi = \phi_{obs.} - \phi_{théor.}$ représente la différence des phases entre les ondes de marées observées et théoriques qui peut être utilisée pour l'étude de la viscosité de la Terre.

En outre, ces derniers temps beaucoup d'auteurs [1 à 4] considèrent l'influence sur la valeur γ et $\Delta\phi$ des hétérogénéités locales des couches supérieures de l'écorce de la Terre. Ayant en vue cette possibilité, pour observer une fracture d'après les variations de γ et $\Delta\phi$ nous avons soumis à l'analyse harmonique par la méthode Venedikov les données clinométriques observées de 1972 à 1980 dans la galerie de la rive droite n° 183.
Cette galerie coupe une fracture traversant dans la base de la digue d'Ingouri ⌠∋⊂ et les points d'observation y sont répartis sur les blocs A et B séparés par la fracture.

Pour la période indiquée, pour la réduction des quatre appareils n° 34, 14, 101, 107 installés dans la dite galerie, des observations d'une durée générale de 3504 jours étaient disponibles. On a fait en tout 95 analyses mensuelles indépendantes. On a obtenu les valeurs γ et $\Delta\phi$ pour les cinq ondes de marées principales; diurnes O_1 et K_1 et semi-diurnes M_2, S_2 et N_2 qui ont des amplitudes théoriques maximales à la station d'Ingouri (table 1).

Les résultats de la réduction sont donnés dans la table 2. Nous noterons que malgré la grande profondeur de la galerie, la proximité de travaux de construction a déterminé quand même dans les données observées un haut niveau de bruits tecnogènes.

C'est pourquoi nous utiliserons pour l'analyse les valeurs γ et $\Delta\phi$ de l'onde semi-diurne lunaire principale M_2. En comparant les valeurs numériques de $\gamma(M_2)$ pour les quatre appareils obtenues par moyennisation vectorielle d'après les séries indiquées dans la table 2 nous sommes convaincus que dans celles-ci on n'a découvert aucune valeur anormale indiquant une influence de la fracture comme cela a été noté dans la bibliographie [3, 4]. Il est possible de l'expliquer par deux causes. D'abord, les points d'observation ne sont pas en position directement sur la fracture et restent à 10 et 15m de celle-ci. Ensuite, comme cela a été établi en [6] cette fracture ne constitue pas un renforcement actif des déformations de marées et entre les blocs il ne se

produit pas de mouvements tectoniques différentiels sensibles. Dans les valeurs $\gamma(M_2)$ on n'a pas découvert, dans les limites des erreurs de leur détermination, d'inégalité du facteur d'amplitude dans la direction N.S et E.W (table 2).

Comme on le constate par cette table les valeurs du déphasage $\Delta\phi$ pour l'onde M_2 ont le signe positif ce qui témoigne d'une avance de la marée observée par rapport à celle calculée théoriquement. Le signe moins en $\Delta\phi$ pour l'appareil 34 (EW) se trouvant sur le socle avant dans la galerie peut s'expliquer par le fait que le massif montagneux dans lequel est creusée la galerie est situé de telle sorte que seule la composante EW peut être perturbée par les déformations thermiques.

En comparant les valeurs du paramètre γ avant et après le début du remplissage du réservoir d'eau on observe une variation: la valeur de γ après le remplissage est plus petite qu'avant son début. Donner une explication à ce fait ne paraît pas possible à présent. Nous analysons maintenant les données des observations également pour d'autres galeries. Nous espérons que l'examen comparatif de ces données donnera la possibilité d'étudier plus à fond les données de l'analyse harmonique.

Références

1. П. С. Матвеев. Сб. «Вращение и приливные деформации Земли», вып. I. Киев, 1970, 72—86.
2. В. Бухгейм. Сб. «Симпозиум по обмену опытом наклонометрических наблюдений». Л., 1968, 132—155.
3. В. И. Старков, Е. Я. Старкова. Сб. «Вращение и приливные деформации Земли», вып. I. Киев, 1970, 241—249.
4. А. Е. Островский, В. И. Старков, Е. Я. Старкова. Сб. «Изучение земных приливов», М., 1980, 182—188.
5. А. П. Венедиков. Сб. «Симпозиум по обмену опытом наклонометрических наблюдений». Л., 1968, 66—92.
6. Б. К. Балавадзе, В. Г. Абашидзе и др. Сообщения АН ГССР, 98, № 3, 1980, 573—576.

Table 1 Amplitudes théoriques (en ms) des ondes de marées principales calculées pour la station d'Ingouri

Direction	M_2	S_2	N_2	K_1	O_1
E - W	11,58	5,39	2,22	6,21	4,41
N - S	7,83	3,65	1,50	0,78	0,55

Table 2 Valeur de γ et $\Delta\phi$ des ondes de marées principales d'après les observations dans la région d'Ingouri ГЭС, dans la galerie n° 183.

Endroit de l'Observation	Epoque des observations, nombre de jours et de séries	Clinomètre photoélec-électrique	M_2	N_2	S_2	O_1	K_1
			γ, $\Delta\varphi^0$	γ, $\Delta\varphi^0$	γ, $\Delta\varphi^0$	γ, $\Delta\varphi^0$	γ, $\Delta\varphi^0$
Point I jusqu'à la fracture géostructure bloc B	1972-1979 758 jours 19 séries	n° 34 E - W	0,7447 ± 190 —6,5644 ±1,4642	0,7673 ± 586 1,1662 ±4,3558	0,7246 ± 281 —2,4233 ±2,2208	0,4624 ± 526 —16,7101 ±6,5162	0,4210 ± 409 —11,8854 ±5,5625
	1972-1979 534 jours 15 séries	n° 14 N - S	0,7546 ± 232 3,7472 ±1.5428	0,8221 ± 849 —1,1566 ±5,9148	0,7312 ± 466 —4,4883 ±3,6550		
Point II après la fracture géostructure bloc A	1973-1980 1376 jours 36 séries	n° 101 E - W	0,7514 ± 104 4.6620 ±0,7956	0,7445 ± 403 5,6606 ±3,0991	0,5940 ± 152 1,2087 ±1,4654	0,3452 ± 354 —6,8424 ±5,8711	0,4023 ± 408 —6,0346 ±5,8137
	1972-1980 836 jours 25 séries	n° 107 N - S	0,7236 ± 144 2,0474 ±1,1379	0,7936 ± 538 1,3698 ±3,8812	0,7029 ± 307 —16,1387 ±2,4989		

THE KELVIN CALIBRATION MACHINE FOR TILT.

A Contribution to the history of experimental Earth Tides Measurements.

P. Melchior
Observatoire Royal de Belgique

A major concern in experimental measurements is the correct calibration of the instruments in use. The problem consists, in principle, of artificially producing the natural phenomenon one wants to evaluate.

In the case of tilt measurements made with clinometers the solution was given by J. Verbaandert who invented the dilatable bearing plate (crapaudine) and calibrated it using the interferometric method (Verbaandert 1967, see also Ducarme 1988).

The use of such dilatable bearing plates was automated and extended to many stations using VM quartz horizontal pendulum or other similar equipment.

The automatic calibration was a step response of the clinometer to a change of pressure inside the bearing plate produced automatically twice a week (Melchior 1996 - figures 43 to 48 and Melchior 1983 - figures 8.10 to 8.15).

In early 1964 I became concerned with the problem of the frequency response of the pendulum to artificial periodic variations of pressure inside the bearing plate. To address this issue I constructed a kind of Kelvin tidal prevision machine with a limited number of components whose periods were chosen outside the tidal frequency bands.
I thus selected three periods incompatible with each other and with tidal periods as well : 7 hours, 17 hours and 37 hours which were injected in crapaudines to add a permanent artificial tide with 3 components to the natural tides.
The machine was manufactured by the BETEA factory in Bruxelles.
Each pulley and the summation disk were equipped with a potentiometer (linearity 0.1%) and was activated by a 5 watt synchronous motor.
The periods of rotation of these motors were 6h, 24h and 24h which were combined with mechanical gears gave the pulleys periods of respectively 7h, 17h and 37h. Potentiometers readings were taken every hour.
A thorough critical examination of all mechanical and electronic parts of the machine was performed by the late B. Georis and is given in full detail in his licence thesis in physical sciences, Louvain University 1967.

The amplitude of each periodic oscillation can be chosen just as in a Kelvin machine. The sum of the three vertical oscillations is obtained through the up and down movement of a flat tempered steel ribbon successively passing over each of the three moving pulleys (X, Y, Z), and over the three fixed pulleys (L, M, N). The larger disk L is marked with graduations to indicate the phase. The mercury level is suspended on the end of the ribbon (as shown on figure 1) and connected by a 5 meter long plastic tube to two crapaudines.

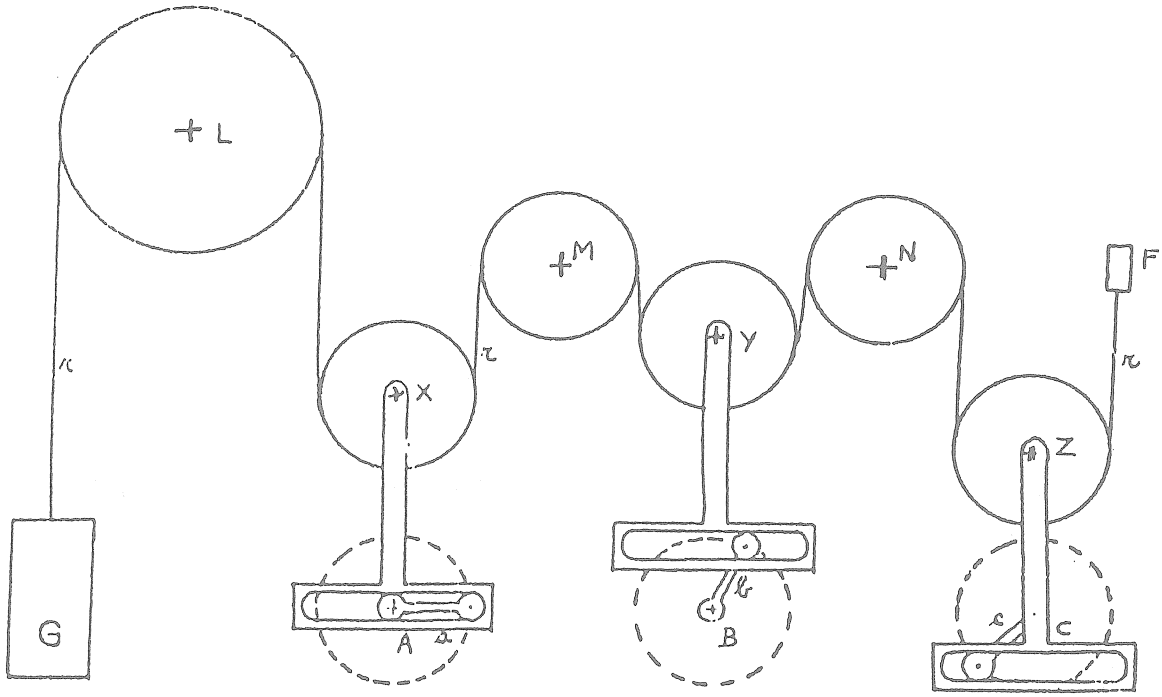

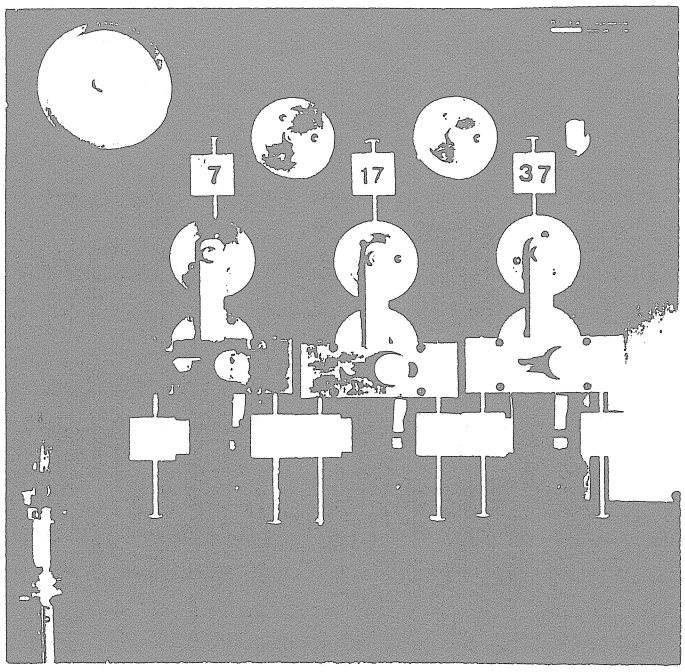

FIGURE 1

TABLE I

ETALONNAGES AUTOMATIQUES PROGRAMMES
WARMIFONTAINE
APPAREIL VM 04 - COMPOSANTE NS
CRAPAUDINE NUMERO 105 - MACHINE DE KELVIN
DENIVELLATION 7H 03.97CM 17H 0.0 CM 37H 07.92CM
ETALONNAGE PAR ONDES FORCEES

INDICATIF	7 HEURES		17 HEURES		37 HEURES	
	AMPL.	PHASE	AMPL.	PHASE	AMPL.	PHASE
68 06 03 00	010.575	221.17	001.543	350.50	022.425	288.004
68 06 08 00	009.158	006.03	000.531	168.59	020.844	190.424
68 06 13 00	009.095	149.24	002.075	033.45	017.071	118.444
68 06 18 00	009.096	287.33	000.668	115.58	017.871	358.534
68 06 23 00	009.071	070.41	000.875	271.79	018.294	255.704
68 06 28 00	009.049	213.89	000.838	020.17	016.841	156.504
68 07 03 00	009.553	354.50	000.683	044.90	015.233	072.074
68 07 08 00	009.051	138.56	000.660	289.79	018.868	324.404
68 07 13 00	009.245	281.30	001.598	108.11	020.910	229.054
68 07 18 00	008.993	064.35	000.987	288.62	020.832	126.884
68 07 23 00	009.173	210.12	000.967	023.78	018.628	028.864
68 07 28 00	008.113	356.40	000.449	180.64	018.647	287.344
68 08 02 00	009.299	148.91	000.880	270.98	016.048	194.624
68 08 07 00	008.966	293.34	000.861	078.79	018.705	101.924
68 08 12 00	009.160	080.88	000.437	243.58	020.183	358.164
68 08 17 00	009.232	217.01	001.427	150.63	020.460	288.004
68 08 22 00	009.141	003.17	000.322	193.98	019.482	165.254
68 08 27 00	009.333	146.57	000.397	305.70	019.334	058.884
68 09 01 00	008.990	289.95	001.291	083.08	019.375	323.904
68 09 06 00	009.216	072.41	001.072	259.23	018.306	225.024
68 09 11 00	009.347	212.54	002.739	141.33	011.555	096.374
68 09 16 00	009.563	357.25	000.881	062.83	013.237	045.814

The machine was put into operation in June 1968 in the station Warmifontaine, Belgian Ardennes, a slate mine at a depth of 150 meters.

The first step in the data analysis was to check the precision of the realisation of the three oscillatory periods and the response of the VM pendulums in conjunction with the amplitudes of the oscillations.

Unfortunately the experiments were limited in time : 3 months in 1968 and 5 months in 1969. Difficulties additionnally arise from very short (or long) power interruptions in the mine which resulted in phase shifts.
Nevertheless two series of nearly continuous registrations were obtained with four different VM pendulums in both the NS and EW fundamental components.
The calibrations carefully performed by B. Georis with a cathetometer indicated that the chosen amplitude for the 7h period was 3.967 ± 0.006 cm, for the 17h period 6.008 cm and for the 37h period 7.918 ± 0.006 cm. But in practice it was zero for the 17h period, due to a failure of the corresponding motor. Table I gives a sample of results obtained in NS component with the pendulum VM04.
Table II shows the obtained response on the photographic registrations in the NS and EW components.

Table II - Response of the VM pendulums

Period (hours)	Kelvin amplitude (cm)	EW component VM30 - 16 values (mm)	NS component VM04 - 22 values (mm)
7.041	3.967 ± 0.006	10.806 ± 0.111	9.187 ± 0.034
17.000	0	1.109	1.008
37.000	7.918 ± 0.006	21.583 ± 0.725	18.325 ± 0.550
ratio 37/7	1.996	1.997	1.995

We checked the accuracy of the imposed periods by making analyses every 120 hours (5 days).

If the periods were absolutely correct, the accumulated phase difference after five days would be, for the 37 hours period :

$5 \times (24h - 37h) = -(13h \times 5) \times 15°/h = -255°$

while 42 differences gives $+ 104.3° \pm 2.4°$

$359.3°$

Thus, considering the rather large dispersion of the observed phases we can consider that the period is exactly 37 hours.

and for the 7 hours period :

$5 \times (24h - 21h) = +15h \times 15°/h = +225°$
while 65 differences gives $+215.9° \pm 0°6$
with a small dispersion $9.1°$

thus the exact period is 7.0405 hours :

$5 \times (24h - 21.1215h) = 14.3925h \times 15°/h = 215.9°$

Only a limited number of monthly harmonic analyses could be performed by the Lecolazet's method.
The results of eight analyses in the NS component and one analysis in the EW component are reproduced in the Table III.
The calibrations were based upon the response of the clinometers to the 7 hour period.
The azimuth of the VM04 pendulum was 6.13° which results, for the semi-diurnal waves in a phase lag of 8.00° compatible with the M_2 and S_2 phases.
The azimuth of the VM30 pendulum was 11.0° which results for the semi-diurnal waves in a phase lag of 8.45° and for the diurnal waves in a phase lag of 2.45°.
Table IV presents an historical example of the IBM 1620 computer output for the Lecolazet procedure. This analysis has been assigned reference number 5317 !
The results of course are only of historical interest.

Acknowledgements :

The dissertation of Baudouin Georis was a model of experimental work by a young promising student who, very unfortunately, died soon after.
Bernard Ducarme cooperated in the analysis of the data.

Table III

Station 0208 Warmifontaine 2 NS Component
Latitude 49°50'N longitude 5°23'E depth 150m

Pendulum VM04, Azimuth 6.13°

Calibration : 7 hour component of the Kelvin machine.

Epoch	M_2 amplitude 0''0050		S_2 amplitude 0''0025	
	γ	α	γ	α
1968 06 18	0.605	- 8.65°	0.679	- 6.52°
06 29	0.623	- 6.66°	0.700	- 8.97°
07 09	0.627	- 8.62°	0.690	- 6.50°
07 20	0.657	- 7.16°	0.722	- 9.45°
07 30	0.668	- 7.88°	0.645	- 6.81°
08 10	0.648	- 8.44°	0.628	- 6.68°
08 20	0.624	- 7.65°	0.619	- 6.03°
08 31	0.654	- 8.43°	0.631	- 6.14°

the amplitudes of the diurnal waves are negligible in NS component at the latitude 49°50'

Station 0208 Warmifontaine 2 EW Component
Latitude 49°50'N longitude 5°23'E depth 150m

Pendulum VM30, Azimuth 11.0°

Calibration : 7 hour component of the Kelvin machine.

Epoch	M_2 amplitude 0''0080		O_1 amplitude 0''0042	
	γ	α	γ	α
1968 06 18	0.667	- 15.50°	0.622	- 3.96°

TABLE IV

CENTRE INTERNATIONAL DES MAREES TERRESTRES

ANALYSE HARMONIQUE NO5317 METHODE LECOLAZET ORDINATEUR IBM 1620

STATION WARMIFONTAINE 2 MACHINE DE KELVIN 07H Z INSTRUMENT PEND.HOR.EW 30

LATITUDE 49 50 N

LONGITUDE 5 23 E EPOQUE 1968 06.18.15

T#2440026125 DT#0,6846167008 N#12

TAU# 316.236669 S# 001.061199 H# 086.917268

P# 240.109107 NPR# 344.988132 P1# 282.398123

ONDES DIURNES ET SEMI-DIURNES

	A_T	$A_0 \times 10$	α_T	α_0	$\gamma \times 10$	κ
K1	97,1641	605,6233	316,4827	308,8768	6,2329	-7,6059
O1	60,8473	378,5866	137,4490	133,4890	6,2219	-3,9600
Q1	13,0149	82,7857	20,1216	354,8308	6,3608	334,7092
M1	3,4167	37,2334	228,4760	146,2534	10,8974	-82,2226
J1	7,1725	29,6690	93,9099	94,6444	4,1364	0,7345
M2	99,6928	664,6033	181,6574	166,1527	6,6665	-15,5047
S2	28,4341	182,6020	15,8210	355,3277	6,4219	339,5067
N2	20,2530	134,7262	64,4066	50,6304	6,6521	-13,7762
L2	5,1221	20,6131	66,7044	89,5981	4,0243	22,8937
ZN2	4,7540	25,3012	322,4342	300,8282	5,3220	-21,6060

A_T calculated theoretical amplitude

A_0 observed amplitude x 10

α_T calculated theoretical phase

α_0 observed phase

Références

Ducarme, B., 1973
Problèmes instrumentaux liés à l'enregistrement et à l'analyse des phénomènes de marée terrestre.
Thèse de doctorat, Université Catholique de Louvain (pages 191 à 195).

Ducarme, B., 1988.
25 Years of Experience with crapaudine at the International Centre for Earth Tides.
Bull. Inf. Marées Terrestres 101 : 7098-7104.

Georis, B., 1967.
Contrôle permanent de la sensibilité des pendules horizontaux.
Mémoire de licence, Université Catholique de Louvain, 119 pages et programmes de calcul.

Kelvin (Lord), 1911.
Mathematical and Physical Papers, vol. VI, Cambridge U.P.

Melchior, P., 1964.
L'évolution des idées et des techniques d'observation dans l'étude des marées terrestres.
Observ. Roy. Belgique. Com. 235, Série Géophysique 68, 32 pages.

Melchior, P., 1966.
Un système d'étalonnage automatique programmé pour les stations clinométriques souterraines.
Bull. Inf. Marées Terrestres 44 : 1707-1709.

Melchior, P., 1983.
The Tides of the Planet Earth, 2nd Edition.
Pergamon Press, 641 pages.

Verbaandert, J., 1960.
Etalonnage des pendules horizontaux par crapaudine dilatable étudiée interférométriquement.
3è Symp. Marées Terrestres, Trieste.
Boll. Geofisica Teorica e Appl. 2 : 81-90.